AN ABSTRACT OF THE THESIS OF

Evangelos Metaxides for the degree of Master of Science in Mechanical Engineering presented on March 10, 1995. Title: Static and Dynamic Testing of a Recumbent Bicycle's Suspension Components, and Design of a Damping Coefficient-Spring Constant Test Machine.

Redacted for Privacy

Abstract approved: _____

David G. Ullman

The purpose of this study is to provide the necessary technical background and data for the development of a suspension system for a recumbent bicycle. For this reason, the customer requirements-design criteria for the development of the suspension system were set, and several static and dynamic tests were conducted on the bicycle's suspension components in order to determine their shock absorption properties. The shock absorption properties of the bicycle's components can be used as means of evaluating the specifications of the suspension system that will satisfy the established design criteria best. In addition, a test machine that can be used for damping coefficient and spring constant measurements was designed to provide further assistance with the analysis of the damping and elastic properties of the recumbent bicycle's suspension components. It was designed so that it can also be used for similar testing of other materials and parts used in the bicycle industry. The subject of this study was BikeE, a recumbent bicycle that was developed by Professor D. G. Ullman and the BikeE Corporation in 1992.

Static and Dynamic Testing of a Recumbent Bicycle's Suspension Components, and Design of a Damping Coefficient-Spring Constant Test Machine

by

Evangelos Metaxides

A THESIS
submitted to
Oregon State University

in partial fulfillment of
the requirements for the
degree of

Master of Science

Completed March 10, 1995
Commencement June 1995

Master of Science thesis of Evangelos Metaxides presented on March 10, 1995

APPROVED:

Redacted for Privacy

Major Professor, representing Design

Redacted for Privacy

Acting Chair of Department of Mechanical Engineering

Redacted for Privacy

Dean of Graduate School

I understand that my thesis will become part of the permanent collection of Oregon State University libraries. My signature below authorizes release of my thesis to any reader upon request.

Redacted for Privacy

Evangelos Metaxides, Author

To my mother, and my Aunt Eleni

TABLE OF CONTENTS

TABLE OF CONTENTS (CONTINUED)

TABLE OF CONTENTS (CONTINUED)

LIST OF FIGURES

LIST OF FIGURES (CONTINUED)

LIST OF TABLES

Static and Dynamic Testing
of a Recumbent Bicycle's Suspension Components, and
Design of a Damping Coefficient-Spring Constant Test Machine

1. INTRODUCTION/BACKGROUND TOPICS

1.1 BACKGROUND OF RECUMBENT BICYCLES

Recumbent bicycles are two-wheeled, pedal-powered vehicles with the rider in a seated position that can range from nearly upright to steeply reclining. The advantages of the recumbent position over the standard bicycle position are superior rider comfort and efficiency. Due to its ergonomic design, that ensures a natural, upright seated position for the rider, there is little strain on the back and the arms can rest on the handle bars at mid-chest height. Moreover, on traditional bicycles the rider looks down at the road, whereas on recumbents, the passing world and traffic are easily seen. The superior aerodynamic position of the rider on recumbent bicycles also provides less wind resistance than that experienced by a traditional bicycle rider. It comes as no surprise that recumbents now hold all bicycle land speed records.

1.2 THE HISTORY OF BIKEE

BikeE (illustrated in Figures 1 & 2) is a recumbent bicycle that was developed by the BikeE Corporation, a company founded by Paul Atwood, Richard Rau, and Dr. David Ullman of Oregon State University.

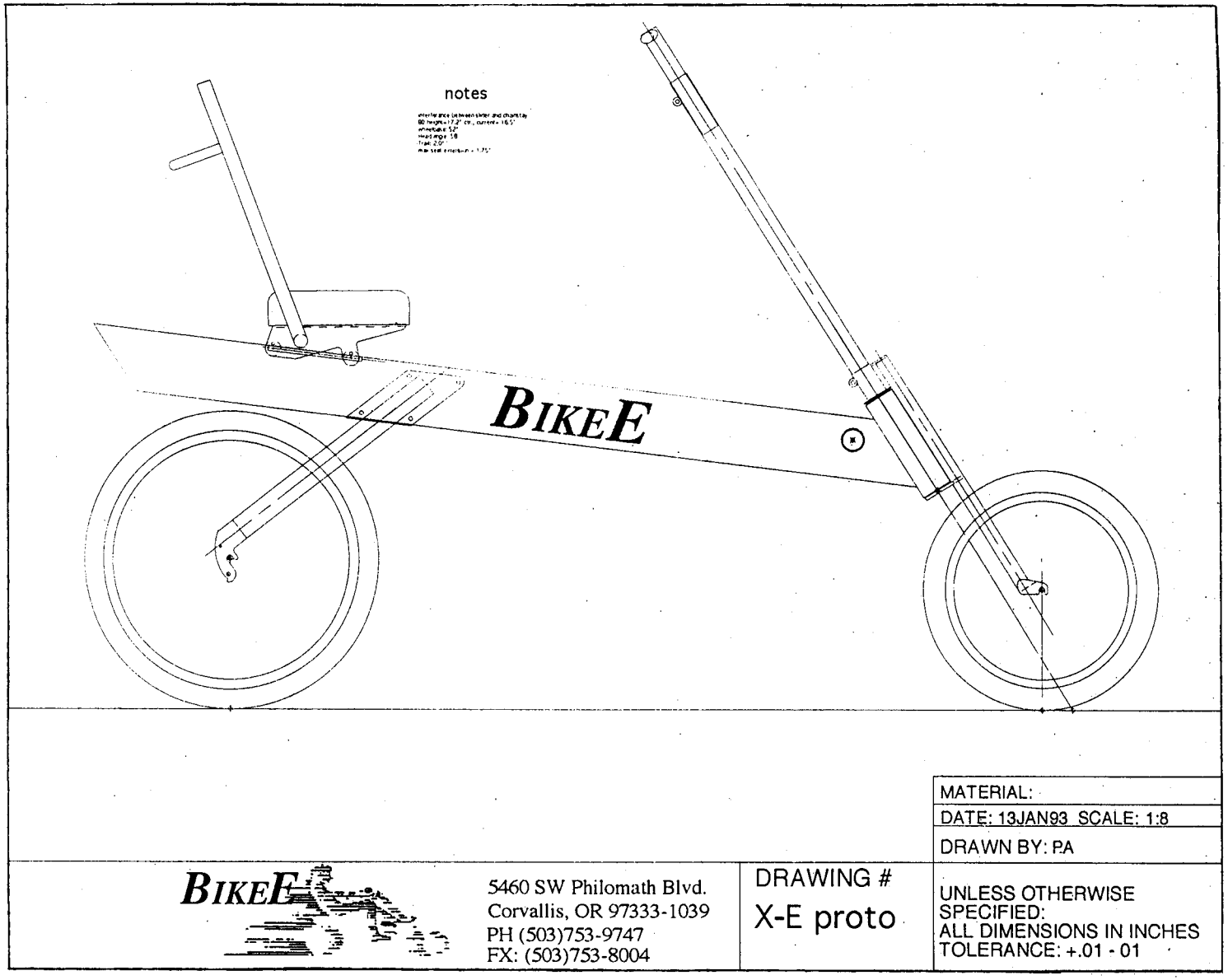

FIGURE 1 BikeE.

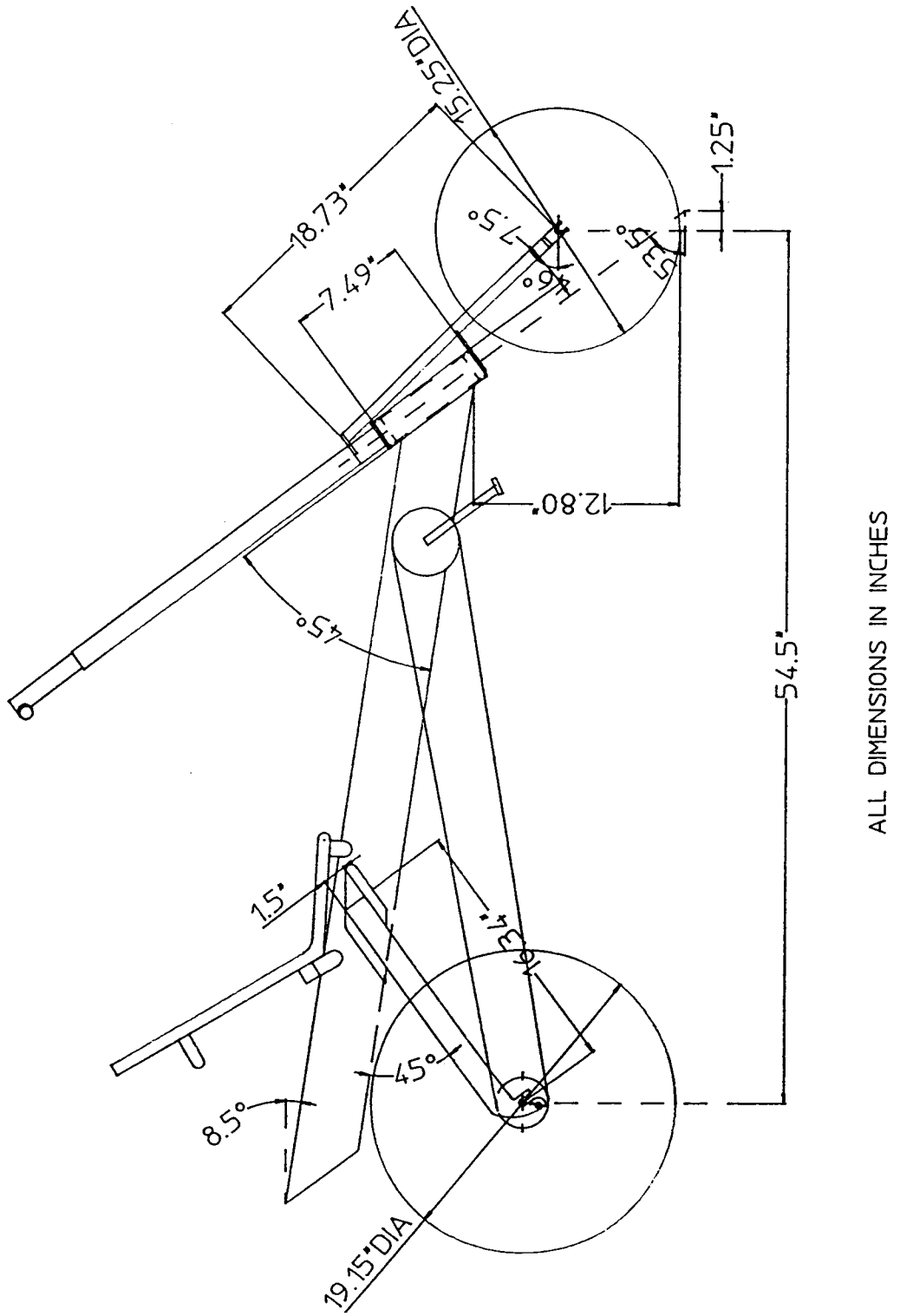

FIGURE 2 BikeE's dimensions.

Its founders combined their love for cycling, their knowledge of the bicycle industry, as well as their expertise in product design and development, creating a successful blend of industry and academia. By setting all the requirements for creating a type of bicycle that would provide significantly higher rider comfort, they paved the road for BikeE's development. The development of BikeE began in summer of 1992 and a pre-production prototype was completed in November of the same year.

In addition to all the advantages of recumbent bicycles over conventional models, BikeE enjoys the following features: It is

- comfortable to ride
- easy to ride
- affordable
- of high quality
- simple to manufacture, assemble, and maintain
- appealing to bicycle retailers
- modular

More important, the modular nature of BikeE has allowed the designers/manufacturers the flexibility of being able of not only continuously improving the initial product, but easily adding accessories and new components that would enhance the bicycle's performance. So over the past few years a new, improved BikeE configuration that is lighter, less expensive to manufacture, handles better, and will fit most of the riding population has been developed. Furthermore, several accessories like a speed kit, a touring kit, a foul weather kit, a fairing kit and a trunk kit have also been introduced. The latest accessory that BikeE's manufacturers plan to develop is a suspension system that will significantly

increase shock absorbtion and thus improve ride smoothness. The purpose of this study is to provide the necessary data that will allow the determination of the suspension system's desired specifications, assisting the design process in the development of an efficient and scientifically sound product.

2. INITIAL STAGES OF THE DESIGN PROCESS

One of the most immediate goals of BikeE Corporation is, as mentioned earlier, the design and development of a suspension system that would enhance BikeE's shock absorbtion and ride smoothness. The aim of this section is to explore and describe the initial stages of this design project.

2.1 PERFORMING A QUALITY FUNCTION DEPLOYMENT ANALYSIS (QFD) ON BIKEE'S SUSPENSION SYSTEM DESIGN

The most critical part of the design process is to accurately define the design problem at the beginning, and try to understand what exactly is asked to be done. The goal in understanding the design problem is to be able to follow as close as possible the four following steps:

Step 1: determine the customers involved in the design and development process

Step 2: define the corresponding customer requirements

Step 3: determine the relative importance of the customer requirements

Step 4: translate the customer requirements into engineering requirements, i.e. a technical description of the goals that need to be achieved (Ullman, 1992.)

In designing a suspension system for BikeE the four steps described above were used as the principal guidelines for the design process.

First the customers were determined:

- the consumers

- the BikeE Corporation employees (management, manufacturing, assembly, sales and advertisement personnel)
- bicycle-shop owners and repair personnel
- transportation servicemen
- disposal specialists

Second the customer requirements were defined based on considerations of the suspension system's functional performance, the human parameters involved, the system's physical requirements and reliability, its life cycle and available production resources. A consultation with BikeE's manufacturers has assisted in refining the customer requirements and deciding that the desired suspension system needs to:

1] absorb bump vibrations (mainly for bumps smaller than 1.50", with special attention to the most ordinary ones of 0.25" or smaller size)

2] not affect the bicycle's control

3] be safe during operation

4] be attractive

5] be easy to understand and operate

6] be adjustable to the rider's weight

7] be adjustable for ride stiffness

8] have a low weight

9] not rattle during operation

10] keep the wheels aligned

11] not interfere/affect the rider

12] not interfere/affect other parts of the bicycle

13] not interfere with the terrain

14] have a long life span (at least as long as the bicycle's)

15] be easy to attach

16] be fast to attach

17] be easy to repair

18] be easy to maintain

19] have few parts

20] be easy to find spare parts

21] be easy to assemble

22] operate in all types of weather and temperature

23] be unaffected by dirt

24] be unaffected by humidity

25] be unaffected by very frequent use

26] be unaffected when unused for a long time

27] be of low cost

28] be recyclable - environment friendly

29] be easy and fast to manufacture

30] be easy and safe to store

31] easy and safe to transport

The next step in these initial stages of the design is, as mentioned above, to determine the relative importance of the customer requirements. This is accomplished by assigning a weighting factor in a scale from 1 to 10 to each requirement. Each requirement's individual weight will be indicative of the effort, time and money that is worth consuming on trying to achieve it. The customer requirements that are assigned the maximum possible weight of 10 are the absolutely essential requirements without which the design is meaningless.

It was mentioned at the beginning of this section that the most critical stage of the design process is the initial one, during which the designer has to understand what exactly the design problem is and what exactly is asked to be done. Following the guidelines (steps 1-3) described

above is the first step to the right direction. However, although they provide valuable information about the design problem, the nature of these guidelines is rather abstract. On the other hand, step 4 (translation of the customer requirements to engineering requirements) calls for a lower level of abstraction in the getting-to-know-the-problem process as a more refined technical description of the goals that need to be achieved is required. Thus, before step 4 is undertaken, a deeper understanding of the problem, this time in technical terms, would not only be useful but essential as well. In order to obtain the necessary technical data that would allow the successful design of a suspension system for BikeE, a series of tests were run on the existing model as described in the chapter that follows.

2.2 CREATING A DECISION MATRIX

The customer requirements/design criteria that were defined in the previous section, along with their corresponding assigned weight, were also organized for future use in the form of a table that can serve as the suspension system's decision matrix (Figure 3). The role of a decision matrix is to provide the designer with a simple, yet effective, method to evaluate different design concepts, and help the latter decide which one presents the highest potential for a successful product design.

	BIKEE's SUSPENSION SYSTEM DECISION MATRIX	WEIGHT (scale 1-10)	CONCEPTS TO BE COMPARED						
			I	II	III	IV	V	VI	VII
C	Absorb vibrations for bumps <=0.25"	10							
U	Absorb vibrations for bumps >0.25", <=1.5"	8							
S	Absorb vibrations for bumps >1.5"	4							
T	Does not affect control	10							
O	Safe during operation	10							
M	Attractive design	8							
E	Easy to understand and operate	10							
R	Adjustable to rider's weight	9							
	Adjustable to ride stiffness	9							
R	Low weight	8							
E	Not rattle during operation	9							
Q	Keeps wheel aligned	10							
U	Does not interfere/affect rider	10							
I	Does not interfere/affect other parts	10							
R	Does not interfere with terrain	10							
E	Long life span (at least as long as bike's)	9							
M	Easy to attach	8							
E	Fast to attach	8							
N	Easy to repair	7							
T	Easy to maintain	7							
S	Few parts	8							
	Easy to find spare parts	6							
/	Easy to assemble	8							
	Operate in all types of weather/temp.	10							
C	Unaffected by dirt	9							
R	Unaffected by humidity	9							
I	Unaffected by very frequent use	6							
T	Unaffected when unused for long time	8							
E	Low cost	9							
R	Recyclable - Environment friendly	6							
I	Easy and fast to manufacture	8							
A	Easy and safe to store	7							
	Easy and safe to transport	7							
E	OVERALL SCORE	**TOTAL +**							
V		**TOTAL -**							
A		**NET TOTAL**							
L	WEIGHTED SCORE	**TOTAL +**							
U		**TOTAL -**							
A		**NET TOTAL**							
T									
I									
O									
N									

FIGURE 3 Decision Matrix for BikeE's suspension system.

3. DATA ACQUISITION

3.1 OVERVIEW OF THE DATA ACQUISITION PROCESS

It was mentioned earlier that an essential part of the designing process for developing a suspension system for BikeE was the need to obtain the technical data about the existing model that would allow a better understanding of what the design target is and how this target is to be achieved. In doing so, two questions arose. First, what kind of data about the existing model was desired, and second, how this data was going to be obtained.

The answer to the first question was relatively simple: what needed to be known was how the existing model behaves under road bump excitation, i.e. what the recumbent bicycle's effective damping coefficient and spring constant are. However, the bicycle is not a solid unit whose characteristic values can be easily measured; it is an assembly of several components with different individual characteristics as both their damping and flexibility are concerned. Thus, an accurate description of the bicycle's response to road excitation would require the knowledge of the technical data (namely the spring constants and the damping coefficients) of its individual components. Although the complexity of the bicycle assembly and the number of the individual components that constitute it are up to the designer, a system of three major components, the bicycle's rear wheel, its frame and its seat/rider is adequate for the desired design analysis purposes. Hence, BikeE was viewed as a system of three (wheel, frame, seat) spring-dampers in series, one on top of the other, whose spring constants and damping

coefficients needed to be known.

The answer to the second question, now, as to how the technical data described above is to be obtained is explicitely given in the next chapter. The rear wheel's and frame's spring constants were first found by studying the bicycle's vertical deflection under load at several points. Then, the strains experienced by the bicycle's different components under load were examined, allowing a cross-check of the wheel's and frame's spring constants as well as providing some information on the stresses and strains that the suspension system would be subjected to. Furthermore, the rear wheel's damping coefficient was determined by measuring its rebound height after a recorded height drop; the spring constants for different seat materials were also measured by studying their deformation-deflection under load. Finally, an overall response of the bicycle to a 0.75" bump simulation was experimentally obtained.

3.2 VERTICAL DEFLECTION OF THE BICYCLE UNDER LOAD

3.2.1 Introduction

The first experiment that was conducted as part of the testing of BikeE's existing suspension system was designed to measure the deflection under load of

a) the bicycle's rear wheel axle, and

b) the whole bicycle at a point on its frame directly above the rear wheel's axle.

The experimentally obtained data on the bicycle's vertical deflection was,

then, compared to the theoretically predicted values.

The major goal of this experiment was the calculation of the spring constants of a) the rear wheel (including the tire), b) the rear wheel-frame system, and c) the bicycle's frame; these were in turn compared to the theoretically predicted values as well.

3.2.2 Procedure

The front wheel of the bicycle was removed, and its front fork was properly mounted and secured on a testing apparatus developed by Professor David Ullman to simulate real road surface conditions. This apparatus consists of a front metal bar for bolting down the bicycle's front fork and a rear, belt-driven cylinder with removable "bumps" where the back wheel rests. Two dial indicators, mounted on a vertical steel rod, were used to conduct the experiment, placed at two different points (A and B) on the bicycle as shown in Figure 4. One measured the rear wheel's axis vertical displacement (point A) right under its mounting bolt, while the other one measured the total vertical displacement of the bicycle (point B) right under a 90^0 cornered 1"x3" piece of aluminum plate that was directly attached and extending 1.5" out of the bicycle's frame. The experimental set-up is illustrated in Figure 4.

The seat of the bicycle was removed during the experiment, since earlier trial runs indicated that the seat cushion greatly alters the experimental results as it does not allow the load to properly balance on the bicycle's frame. Then, different weights (0 to 125 lb, in steps of 25 lb) were placed on the bicycle (carefully positioned in the middle of the seat frame to avoid unbalance errors), and the corresponding vertical deflections at points

A and B were recorded at the same time.

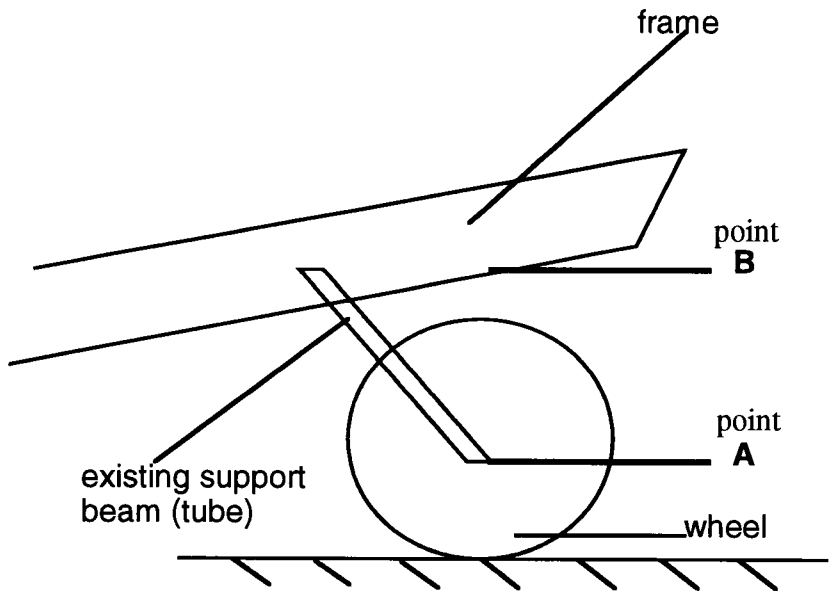

FIGURE 4 Experimental set-up for measuring BikeE's deflection under load.

The experiment was repeated two more times. The rear tire pressure when the experiment was conducted was approximately 35 to 40 psi.

3.2.3 Results

The experimental results obtained are displayed in the following tables:

LOAD (lb)	TRIAL 1	TRIAL 2	TRIAL 3
0	0	0	0
25	0.0630	0.0616	0.0602
50	0.1235	0.1173	0.1160
75	0.1800	0.1711	0.1690
100	0.2360	0.2215	0.2195
125	0.2835	0.2690	0.2664

TABLE 1 Wheel deflection in inches.

LOAD (lb)	TRIAL 1	TRIAL 2	TRIAL 3
0	0	0	0
25	0.0657	0.0660	0.0655
50	0.1288	0.1305	0.1290
75	0.1879	0.1920	0.1880
100	0.2445	0.2482	0.2438
125	0.2974	0.3003	0.2971

TABLE 2 Wheel-frame deflection in inches.

3.2.4 Conclusions and Discussion of results

The first step in the analysis of the experimental results was to illustrate them graphically. Hence, the data presented in tables 1 and 2 above was respectively plotted, and the following two deflection graphs were obtained:

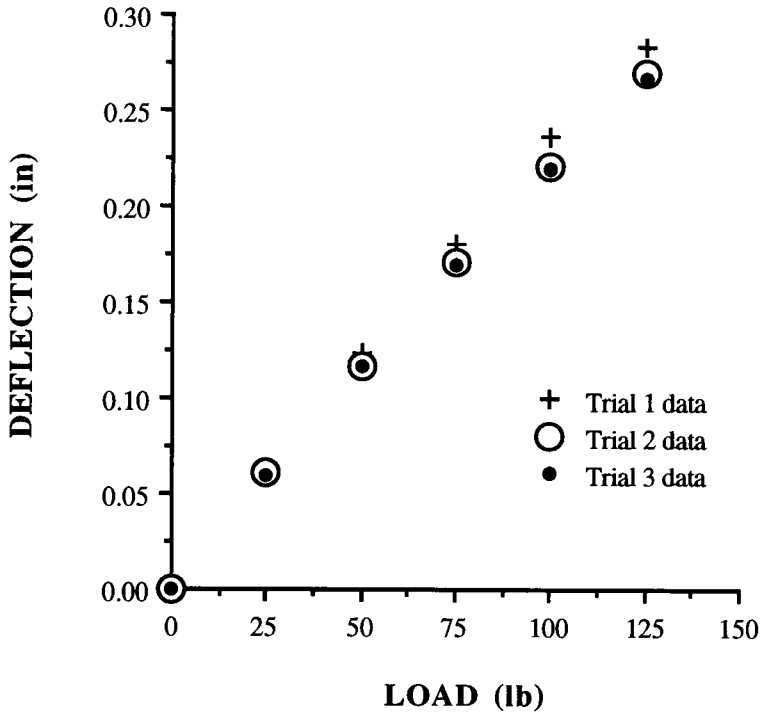

FIGURE 5 Wheel deflection vs load.

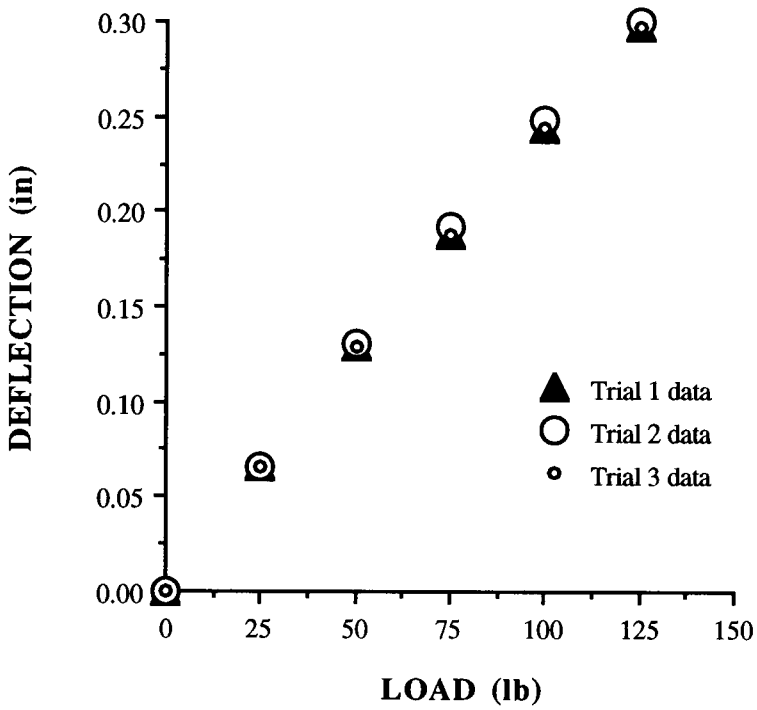

FIGURE 6 Frame-wheel deflection vs load.

The best-fit-line equations (one for each set of experimental data) were, then, derived by the graphics program. These equations allow us to calculate the spring constant (inverse of the slope) of the wheel (including the tire), K_W, and the spring constant of the whole wheel-frame system, K_S. The results are tabulated below:

TRIAL	Kw (lb/in)	TRIAL	Ks (lb/in)
1	469.7	1	420.8
2	465.8	2	420.2
3	439.1	3	414.8

TABLE 3 Experimental spring constant values

From these results, it can be calculated that the mean experimental value and standard deviation for the wheel spring constant, K_W (exp), is

458.2 +/- 16.7 lb/in; similarly, the mean experimental value and standard deviation for the spring constant of the wheel-frame system, K_S (exp), is 418.6 +/- 3.3 lb/in. These results are summarized in table 4 below:

mean Kw (exp.)	mean Ks (exp.)
458.2 +/- 16.7 lb/in	418.6 +/- 3.3 lb/in

TABLE 4 Mean experimental results with standard deviation.

The comparison, now, of the experimentally obtained data with the theoretically predicted values is performed through a comparison of the experimental with the theoretical spring constant values rather than the actual vertical deflections for the following reason: a theoretical calculation of the vertical displacements would require the calculation of the exact force exerted on the beam, something which would add more error and decrease the accuracy of the results.

As no theoretical value for BikeE's rear wheel spring constant is available yet, a theoretical value for the bicycle frame's spring constant can be calculated to assist in the comparison of the experimental data with the theoretical predictions and, thus, the evaluation of its accuracy. The theoretically predicted spring constant value for the bicycle frame (the rear wheel stay) was calculated based on a model of a cantilever beam with an end load P. Since the deflection, δ, of the axis of such a cantilever beam at the beam's end (maximum deflection), due to the bending strains, is given by (Housner and Vreeland, 1983)

$$\delta = Pa^3/3EI \qquad (3.2.1)$$

and the beam's effective spring constant, K, is

$$K = P/\delta \qquad (3.2.2)$$

it yields that the theoretically predicted value for the bicycle frame's spring constant, K_f (theor), is given by

$$K_f \text{ (theor)} = 3EI/a^3 \qquad (3.2.3)$$

where

a = beam length

E_{steel} = Young's modulus

I = moment of inertia

When the corresponding values for the bicycle's frame system, i.e.

- a = beam length =12.375 in.,
- E_{steel} = Young's modulus (steel) = 30 x 10^6 psi,

and

- $I = [bh^3 - (b - t)(h - t)^3]/12 = 0.032$ lbin^2 (3.2.4)

for the beam's/rear stay's geometry (Housner and Vreeland, 1980), where

h = beam height = 1.500"

b = beam width = 0.750", and

t = beam's tubing = 0.049"

were plugged into equation 3.2.3, the theoretical value for K_f was calculated:

$$K_f \text{ (theor)} = 1519.7 \text{ lb/in.} \qquad (3.2.5)$$

Given, now, the theoretical frame constant from equation 3.2.5 above, K_f (theor), and the mean experimental wheel constant from Table 4, K_W (exp), a semi-theoretical value for the spring constant of the whole wheel-frame system, K_S (pred), can be predicted. This value is derived by applying to K_W (exp) and K_f (theor) the equation that expresses the effective spring constant of a system of two springs in series. Hence,

$$K_S \text{ (pred)} = [K_W \text{ (exp)} \, K_f \text{ (theor)}] \, / \, [K_W \text{ (exp)} + K_f \text{ (theor)}] \qquad (3.2.6)$$

Equation 3.2.6 then yields:

$$K_S \text{ (pred)} = 352.1 \text{ lb/in.} \qquad (3.2.7)$$

The mean experimental spring constant value for the whole frame-wheel system, K_S (exp), was found to be 418.6 +/- 3.3 lb/in as shown in Table 4. That is, the system's mean experimental spring constant is 15% different from the semi-theoretical one predicted by equation 3.2.7 above, which indicates an overall agreement between the experimental findings and the theoretical results. Since this comparison was based on the value of the bicycle frame's spring constant that was predicted by the theoretical model (i.e. K_f (theo) = 1519.7 lb/in from equation 3.2.5), the agreement between the experimental and theoretical results also allows to conclude that the bicycle frame's spring constant, K_f, must be in similar agreement with its value predicted by the theoretical model, K_f (theo).

Three basic remarks can be made about the major sources of error in

the experimentally obtained results that are responsible for any discrepancies between them and the theoretically predicted values:

• Although all measurements during the experiment were repeated several times to ensure the accuracy of the results, some random experimental errors did inevitably occur. Therefore, each measured quantity was assigned an uncertainty value as means of indicating the magnitude of possible experimental error associated with it. The uncertainty assigned to the vertical deflection recordings was +/- 0.0003", while the uncertainty assigned to the loading weights was about +/- 1%, and the uncertainty assigned to dimension measurements was +/- 1/64".

• The exact position-balance of the weights on the bicycle's frame seemed to be very important since it affects the exact force exerted on the connecting beam and, thus, the measured deflection.

• Finally, the age and condition of the dial indicators that were used could have influenced the uncertainty on their readings.

3.3 STRAIN MEASUREMENTS

3.3.1 Introduction

The second experiment that was conducted as part of the testing of BikeE's existing suspension system was designed to measure the maximum stress that develop under load on the steel tubes that currently connect the bicycle's frame with its rear wheel (rear stays.) The experimentally obtained data was, then, compared to the theoretically predicted values. In addition, a comparison between the experimental results and the vertical deflection data that was obtained from the first experiment was performed.

3.3.2 Procedure

Two CEA-06-240UZ-120 strain gages were installed on the left steel tube that connects the bicycle's frame and rear wheel according to the instructions given by the The Measurements Group (1983.) The first one (front gage) was placed, given the tube's geometry, as close as possible to the point of maximum stress and strain concentration as shown in Figure 7,

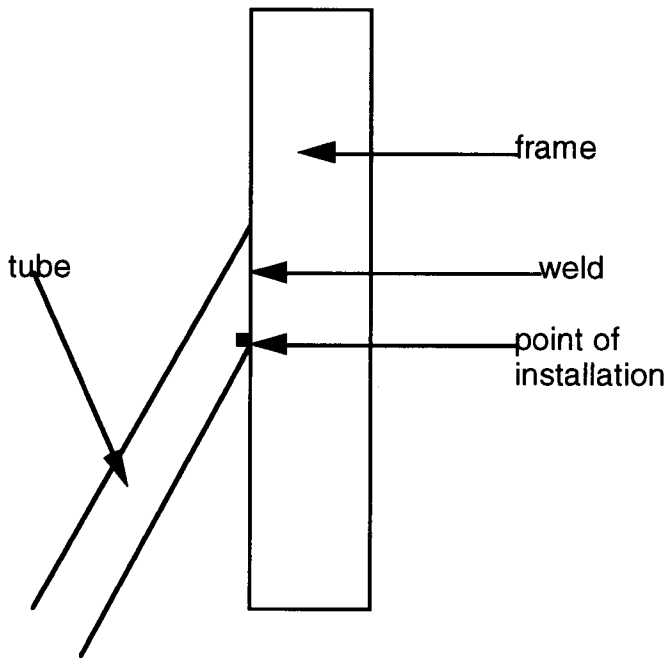

FIGURE 7 Top view of strain gage installation point.

while the second one (back gage) was carefully placed on the tube's opposite surface, symmetrically to the first one.

Lead wires were, then, soldered onto both strain gages and connected to a strain indicator box (3 lead wire bridge configuration.) The seat of the bicycle was again kept off during the experiment, since the seat cushion was

found to add significant errors to the results by not allowing the load to properly balance on the bicycle. Then, different weights (0 to 225 lb, in steps of 25 lb) were placed and properly positioned on the bicycle's frame, and the corresponding strains from both gages were recorded off their respective strain indicator boxes. The experiment was repeated two more times. All the measurements were taken at a rear tire pressure of 35-40 psi.

3.3.3 Results

The experimental results for the front and the back gage are displayed respectively in the two tables below:

LOAD (lb)	TRIAL 1	TRIAL 2	TRIAL 3
O	0	0	0
25	-410	-410	-410
50	-860	-820	-850
75	-1280	-1220	-1270
100	-1660	-1620	-1690
125	-2060	-2020	-2100
150	-2550	-2480	-2450
175	-2970	-2910	-2860
200	-3370	-3320	-3260
225	-3790	-3750	-3650

TABLE 5 Strain recorded by the front gage (in microstrains).

LOAD (lb)	TRIAL 1	TRIAL 2	TRIAL 3
O	0	0	0
25	350	350	360
50	730	700	730
75	1090	1040	1090
100	1410	1370	1440
125	1760	1720	1800
150	2180	2100	2090
175	2550	2470	2440
200	2900	2840	2780
225	3260	3210	3130

TABLE 6 Strain recorded by the back gage (in microstrains).

3.3.4 Conclusions and Discussion of results

The experimental data from tables 5 and 6 above was then plotted, and Figures 8 and 9 below were obtained respectively. Furthermore, in each of these two graphs, in addition to the experimentally obtained results, the respective theoretically predicted curve for the maximum strains developing on the bicycle's rear stay is displayed for comparison. The theoretically predicted curves were generated by plotting the maximum strains that develop at the corresponding points on BikeE's rear tube stays, according to a cantilever beam with an end load model. So,

A] for the front gage

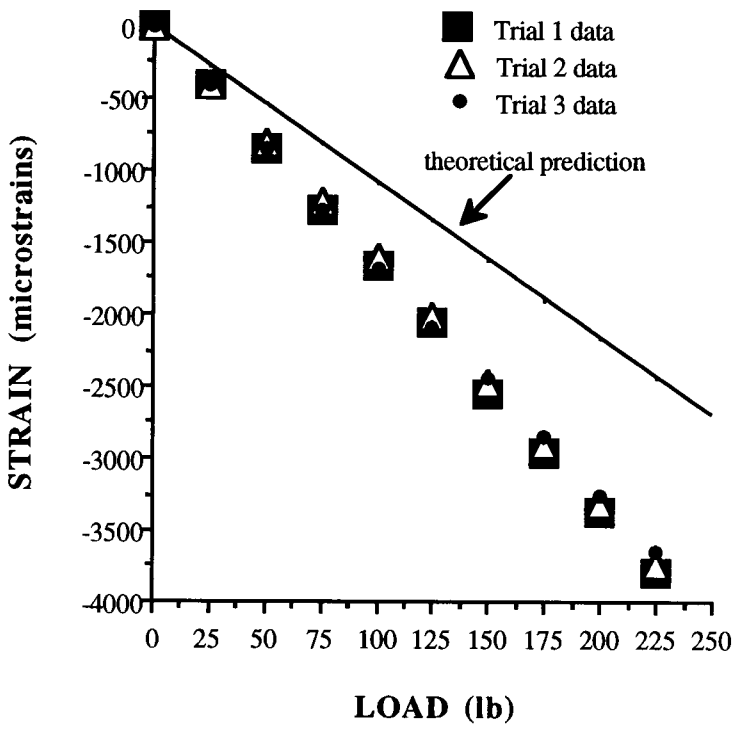

FIGURE 8 Strain measured by the front gage vs load.

B] for the back gage

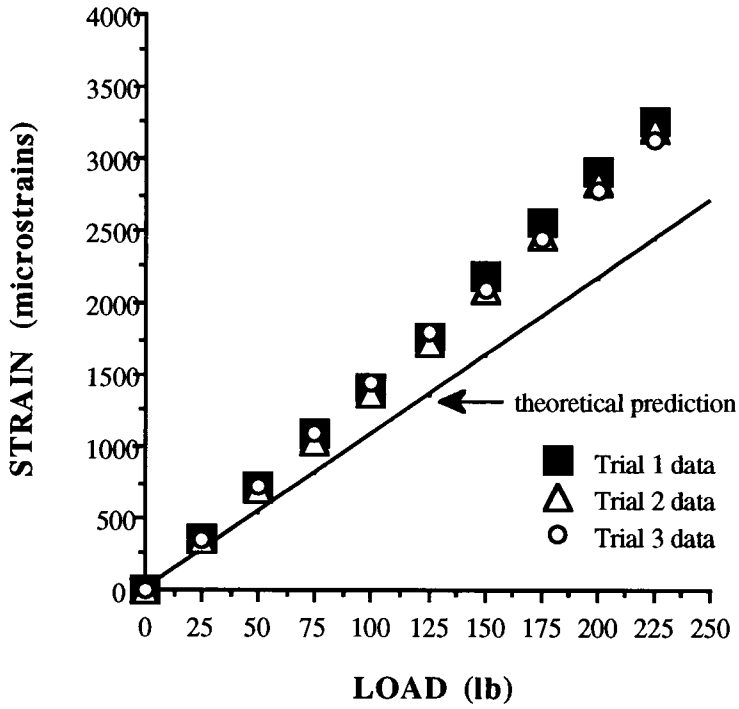

FIGURE 9 Strain measured by the back gage vs load.

As mentioned above, the theoretical analysis of the experiment was based again, as in section 3.2.4, on a model of a cantilever beam with an end load P, and the developing strains were calculated according to the following equation (Housner and Vreeland, 1983)

$$| \varepsilon |_{theor} = P(a - x)y/EI \qquad (3.3.1)$$

where, x and y are the strain gage coordinates; in this case (for BikeE's rear stay geometry, and for a maximum strain analysis):

- x = 0", and y = - 0.75" for the front gage
- x = 0", and y = + 0.75" for the back gage

For the same system, in equation 3.3.1:

E_{steel} = Young's modulus (steel) = 30 x 10^6 psi

a = beam/rear stay length = 12.375 in.

I = moment of inertia of beam/rear stay (from equation 3.2.4)

P = force perpendicular to the beam = cos(45°) x (load)

The strains (absolute values) that were calculated by use of equation 3.3.1 are tabulated below:

LOAD	STRAIN-THEO. (microstrains)
0	0
25	242
50	483
75	725
100	967
125	1208
150	1450
175	1692
200	1934
225	2175

TABLE 7 Theoretically predicted strains (absolute values.)

A comparison between the experimental and theoretically predicted results can be performed through a comparison of the slopes of their respective strain-load curves. This leads to the conclusion that the thoeretically predicted values for the strains that develop on BikeE's existing support (rear stay) are on the average 33% different from the experimentally obtained ones from the front gage in terms of their respective curve slopes (Figure 8), and 21.5% different from the experimentally obtained ones from the back gage, again, in terms of their respective curve slopes (Figure 9). Moreover, there is a 14.6% difference

between the slope of the experimental data recorded by the front gage and the slope of the experimental data recorded by the back gage.

The discrepansies described above between the theoretical predictions and the experimental results, and between the front and back gage recorded data can be attributed to several reasons:

1] In reality, in addition to the force that acts perpendicularly to the beam's (rear stay) axis due to the load placed on the bicycle, there is another component of the vertical load that is parallel to the beam's axis (axial load) due to the beam's orientation (45^o angle) with respect to the bicycle's frame. This axial load, P_a, causes an additional compressive strain, ε_a, that is given by:

$$\varepsilon_a = P_a/AE = (\cos 45^o \times P)/AE = 0.22\ P \text{ microstrains} \qquad (3.3.1a)$$

where

A = rear stay's cross-sectional area (from equation 3.2.4)

P = applied vertical load

Hence, although the effect of axial loading is something that the theoretical model used does not take into account, it accounts for 2.3% of the discrepancy between the experimental and theoretical results, as a direct comparison of equation 3.3.1a with equation 3.3.1 reveals.

2] The uncertainty on the exact location of the weights placed on the bicycle's frame and, thus, on the exact force exerted on the beam each time the corresponding strain measurement was taken.

3] Random experimental errors that result to measurement uncertainties. The uncertainty associated with strain gage recorded data was assigned a value of +/- 1 microstrains, while the uncertainty assigned to the

loading weights was about +/- 1%.

4] Surface irregularities that can affect the precision of strain measurements.

5] Boundary phenomena due to the proximity of the strain gages to the beam's (rear stay) edges that can also affect the precision of strain measurements.

6] Experimental errors due to the fact that the positioning of the strain gages can only approximate and never coincide with the location (point) of maximum stress/strain concentration on the beam (rear stay).

7] Inability to place the two strain gages at precisely symmetric locations on the two opposite surfaces of the beam (rear stay).

Therefore, in general, taking the sources of error explained above into account, the experimental results are in good agreement with the theoretical predictions. What is even more important and encouraging though, is the close agreement between the strain measurement and vertical deflection data described in the following section, as it strongly reinforces the validity of all the experimental results obtained so far.

3.3.5 Comparison of the strain measurement with the vertical deflection measurement results

The use of a theoretical model for experimental results to be compared to is undoubtedly of great assistance as it provides some general indications of whether the experimental findings point towards the right direction. However, real experimental problems and their conditions are inevitably different and more complicated than similar theoretical cases, so a direct comparison of different experimental results on the same (or

similar) subject, obtained at the same laboratory conditions, can provide a more accurate way of measuring the validity of these results. Such a direct comparison can be performed here between the strain measurement data discussed in sections 3.3.3/4 and the vertical deflection data discussed in sections 3.2.3/4, using always, of course, the cantilever beam with an end load model.

Equation 3.2.1, rewritten below, gives the theoretically predicted maximum deflection, δ, of a cantilever beam's axis as explicitely explained in section 3.2.4:

$$\delta = Pa^3/3EI$$

while, as mentioned in section 3.3.4, the theoretically predicted maximum strain, ε, for the system (rear stay/frame) is:

$$\varepsilon = 0.75Pa/EI \qquad (3.3.2)$$

Dividing equation 3.2.1 by equation 3.3.2 yields

$$\delta/P = (a^2/2.25)(\varepsilon/P) \qquad (3.3.3)$$

and, since a = rear stay's length = 12.375 in. for BikeE's rear stay, inverting equation 3.3.3 gives:

$$P/\delta = 0.015(\varepsilon/P)^{-1} \qquad (3.3.4)$$

But, then, equation 3.3.4 can be expressed in terms of the bicycle frame's

spring constant, K_f, as

$$K_f = 0.015(\text{strain-load curve slope})^{-1} \qquad (3.3.5)$$

Thus, by use of equation 3.3.5 it is possible to determine the extent of the agreement between the load-deflection measurements of section 3.2 and the experimental strain data presented here. So, applying equation 3.3.5 to the experimental data recorded by the front and back gage respectively gives:

--> $K_f = 0.015(\text{slope of strain-load curve for the front gage data})^{-1} =$
$= 0.015(\text{slope of graph in Figure 8})^{-1} = 928.6$ lb/in

and

--> $K_f = 0.015(\text{slope of strain-load curve for the back gage data})^{-1} =$
$= 0.015(\text{slope of graph in Figure 9})^{-1} = 1086.7$ lb/in

On the other hand, the load-deflection measurements of section 3.2 revealed a spring constant value of 1519.7 +/- 15% lb/in for the bicycle's frame (page 19), which indicates a consistency between the results of the first two tests conducted on BikeE, especially when the axial loading effects on strain are taken into account.

3.4 EXPERIMENTAL DETERMINATION OF BIKEE'S REAR WHEEL DAMPING COEFFICIENT

3.4.1 Introduction

The goal of this experiment was to determine the damping coefficient of BikeE's rear wheel for different tire pressures, as no recorded data exists

on it. The knowledge of this damping coefficient will be of significant assistance for a better understanding of the existing system as well as for the development of a successful suspension for BikeE.

3.4.2 Procedure

The rear wheel of the bicycle (a 19.15" diameter, 36 spoke wheel with a WEINMANN 2120, 20x1.75 rim, and a KENDA K-154, 20-C-101, 20x1.5 tire) was dropped from 36 inches, and the rebound height was measured several times for a tire pressure of 65 psi . The same procedure was also repeated for tire pressures of 45 and 30 psi, and a graph of the wheel's damping coefficient versus tire pressure was obtained.

3.4.3 Results

The experimental results obtained are displayed in the table below:

TIRE PRESSURE	TRIAL 1	TRIAL 2	TRIAL 3	MEAN with std. deviation
30 psi	28.00	28.00	27.00	27.75 +/- 0.59
45 psi	28.75	28.75	29.25	29.00 +/- 0.31
65 psi	30.50	31.50	31.50	31.25 +/- 0.59

TABLE 8 Rear wheel's rebound height for different tire pressures, in inches.

3.4.4 Conclusions and Discussion of results

After the wheel's mean rebound height was calculated for each tire pressure (as shown in Table 8), the Logarithmic Decrement, δ, of its drop function was found. This was accomplished by means of the following

relationship:

$$\delta = \ln(\text{initial drop height/average rebound height}) \qquad (3.4.1)$$

Then, the damping ratio, ζ, was calculated since

$$\delta = 2\pi\zeta/(1-\zeta^2)^{1/2} \qquad (3.4.2)$$

By definition the damping ratio, ζ, is

$$\zeta = c_W/c_C \qquad (3.4.3)$$

Equation 3.4.3 can be rewritten as

$$c_W = c_C\zeta \qquad (3.4.4)$$

where

- c_W = the wheel's damping coefficient,
- $c_C = 2(K_W m_W)^{1/2}$ is the critical damping, and (3.4.5)
  - m_W = the wheel's mass = wheel's weight/acceleration of gravity = = 3.9 lb/g = 0.12 slugs
  - K_W = 458.2 lb/in from Table 4

Applying the relationships above to the experimental data of Table 8, the damping coefficient of BikeE's rear wheel was calculated for each different tire pressure; the results, along with their respective error bands,

are shown in Table 9:

Tire Pressure	Damping Coefficient, C_W (lb sec/in)
30 psi	0.18 +/- 0.01
45 psi	0.15 +/- 0.01
65 psi	0.10 +/- 0.01

TABLE 9 Damping coefficient of BikeE's rear wheel vs tire pressure.

A graph of the wheel's damping coefficient versus tire pressure was also prepared, as shown below:

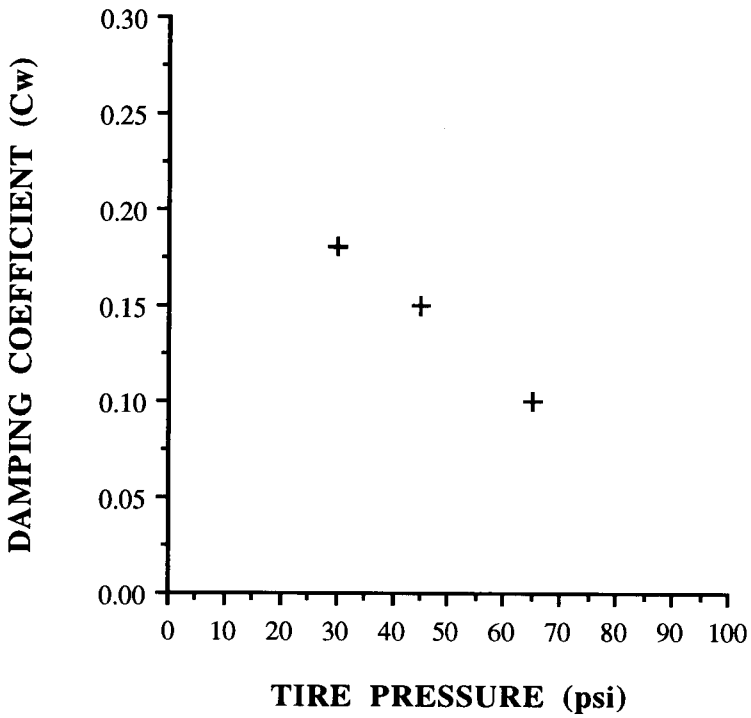

FIGURE 10 Rear wheel's damping coefficient vs tire pressure.

As the graph above indicates, there seems to be a linear relationship

between the wheel's damping coefficient and the tire pressure - at least for the 30 to 65 psi tire pressure range. However, it would be short-sighted to assume that the wheel's damping coefficient exhibits in general only a linear behavior with respect to the tire pressure. Linear behavior is clearly not exhibited in extreme cases as explained below. Consistent with intuitive expectations, Figure 10 suggests that the wheel's damping increases as the tire pressure decreases (the tire gets flatter;) however, it is also easy to understand that as the tire gets flatter, the wheel's damping coefficient will eventually start decreasing as it will then be dominated by the damping coefficient of the rim-spokes system. But, obviously, such extreme cases are not of practical concern. The tire pressure range that is of the most interest is from 30 to 65 psi (everyday use range,) for which, according to the results displayed in Figure 10, it would be safe to assume a basically linear behavior of the wheel's damping coefficient with respect to tire pressure at least until more detailed research results are available.

3.5 EXPERIMENTAL STUDY OF BIKEE's SEAT RESPONSE TO LOAD

3.5.1 Introduction

The purpose of the series of experiments described below was the study of BikeE's seat response/deformation to different load conditions. Samples of both the old and the new seat materials were tested; tests were also performed on the individual foam pads that make up tha seat material in order to determine their response to loading as well. The results of these experiments were used in determining the spring coefficient of BikeE's seat, as part of the general study of the bicycle's response to ride excitation.

3.5.2 Procedure

A 3"x3" sample of BikeE's seat that consists of two layers of foam pads (a 1 1/4" slab of Uniroyal Ensolite "EPC" foam topped with a 3/4" piece of Polyester 4 lb density foam) was placed between two 6.5"x6.5" wooden plates as illustrated in Figure 11. While the bottom plate remained fixed, the top one was able to slide in the vertical direction by means of four thin metal sliders that were press fit to the bottom plate; this experimental device (Figure 11) provided the necessary load balance and stability during the sample's loading, while the effect of friction between

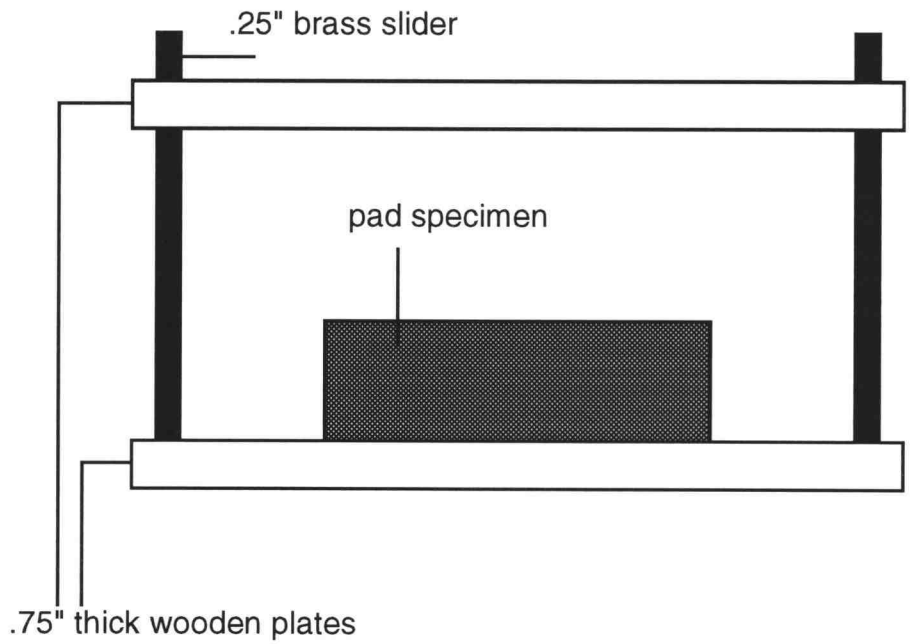

FIGURE 11 Experimental device for measuring seat pad deflection.

the upper plate and the sliders was minimized by allowing an ample tolerance between them. Different weights (ranging from 0 to 30 lb.) were, then, placed on top of the upper wooden plate and its deflection at all four

corners was measured. The average deflection was calculated, the load-deflection results were plotted, and the material's response to load (effective spring constant) was determined. The exact same loading-deformation measurement procedure was also repeated for:

a) the 1 1/4" slab of Uniroyal Ensolite "EPC" foam pad only, and

b) a Polyurethane foam pad suggested for the latest version of BikeE's seat.

3.5.3 Results

The experimental results obtained are shown in the tables that follow:

a) for the original two foam pad layer seat sample

LOAD (lb)	PRESSURE (psi)	TRIAL 1	TRIAL 2
0	0.00	0	0
2.5	0.28	0.0547	
5	0.56	0.0859	0.0937
7.5	0.83	0.3828	
10	1.11	0.5312	0.5234
12.5	1.39	0.6172	0.6250
15	1.67		0.7109
16.5	1.83	0.7109	
20	2.22		0.7734
22.5	2.50	0.8516	
25	2.78		0.8672

TABLE 10 Original two foam pad layer seat's deflection in inches.

b) for the 1 1/4" slab of Uniroyal Ensolite "EPC" foam pad only

LOAD (lb)	PRESSURE (psi)	TRIAL 1	TRIAL 2
0	0.00	0	0
15	1.67	0.2187	0.1875
20	2.22	0.2734	0.2578
25	2.78	0.3359	0.3125
30	3.33	0.3750	0.3672

TABLE 11 Uniroyal Ensolite "EPC" foam pad's deflection in inches.

c) for the Polyurethane foam pad

LOAD (lb)	PRESSURE (psi)	DEFLECTION
0	0.00	0
2.5	0.28	0.0859
5	0.56	0.5547
10	1.11	0.7578

TABLE 12 Polyurethane foam pad's deflection in inches.

3.5.4 Conclusions and Discussion of results

The experimental data from the tables above was respectively plotted and the following deflection graphs were obtained:

1) for the original two foam pad layer seat sample

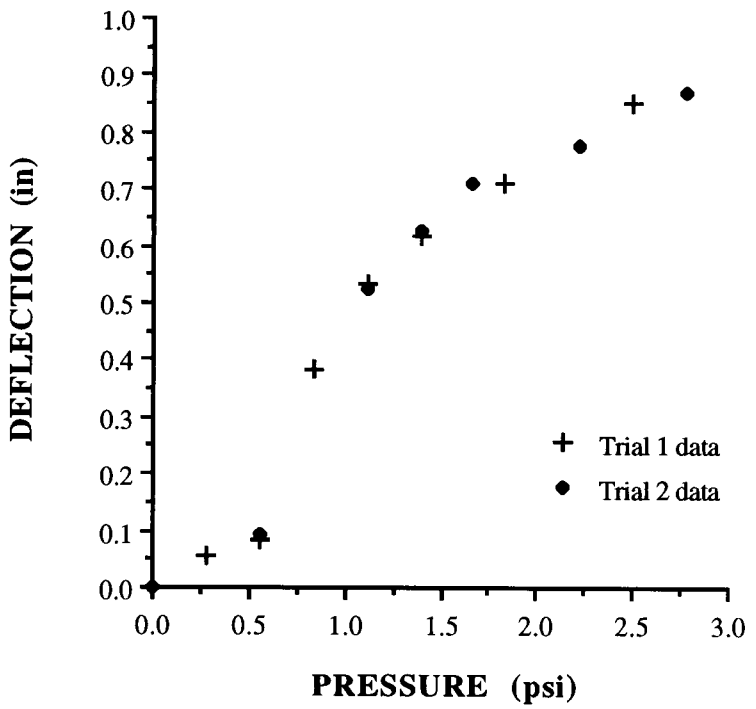

FIGURE 12 Original two foam pad layer seat's deflection vs pressure.

2) for the 1 1/4" slab of Uniroyal Ensolite "EPC" foam pad only

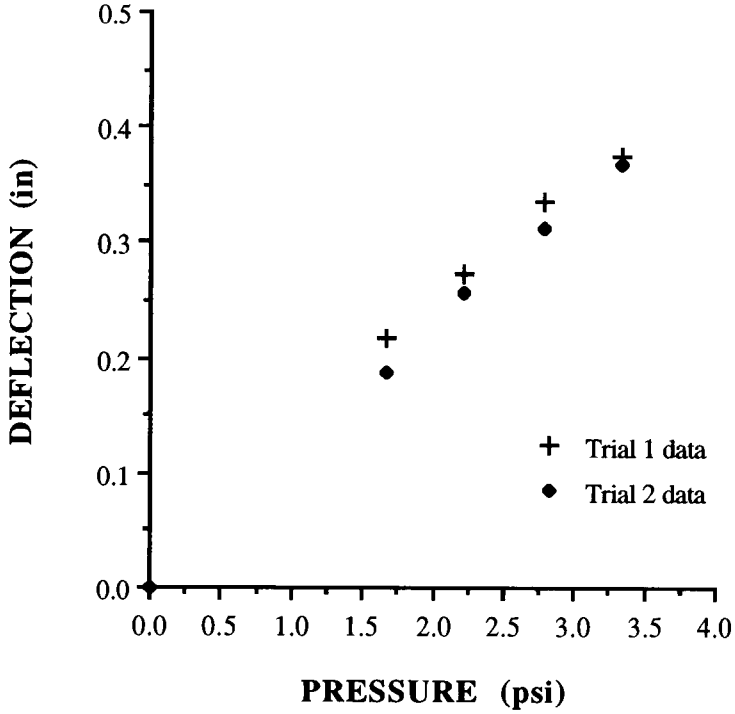

FIGURE 13 Uniroyal Ensolite "EPC" foam pad's deflection vs pressure.

It is evident from Figure 12 that the seat's response to loading follows two steps. Initially, the softer Polyester 4 lb density foam pad responds to the exerted pressure first and deflects almost linearly, until a load of 5 to 6 lbs is reached; then, it gets completely squeezed and has no significant contribution to the seat's vertical deformation. As a result, the thicker and stiffer "EPC" foam pad then picks up and bears the seat's deformation individually. As Figure 12 also suggests, after the thicker "EPC" pad picks up carrying the load (at a pressure of approximately 0.5 to 0.7 psi,) it responds almost linearly to the exerted weight. From the slope of the best fit line generated by the data points recorded for loads over 7 lb, yields that the Uniroyal Ensolite "EPC" foam pad responds with an average spring

constant of 46.6 lb/in in the 0.7 to 3.0 psi pressure range (effective seat spring constant.)

The discussion above suggests that, as the experimental results of Figure 12 indicate, for big loads the seat's effective spring constant is aproximatelly equal to the stiffer "EPC" pad's spring constant. In order to verify this hypothesis, the stiffer pad's response to loading was tested individually. The results are displayed in Table 11 and Figure 13. According to the slope of the best fit line generated by the data points of this graph, the thicker, stiffer "EPC" foam pad deforms, again, almost linearly, but now with an effective spring constant of 84.2 lb/in.

The discrepancy between the two spring constants for the Uniroyal Ensolite "EPC" foam pad that were calculated above can be basically attributed to the following fact: in the first case, although the soft Polyester pad's contribution to the seat's deformation is insignificant after it gets squeezed, it does not stay completely inactive. On the contrary, it still does affect the seat's response to the exerted pressure. Of course, the effect that the Polyester pad has on the seat's response is expected to get smaller and smaller as the loads get higher and it gets even more squeezed. Hence, the discrepancy between the seat's effective spring constant (46.6 lb/in) and the spring constant of the stiffer "EPC" pad (84.2 lb/in) is more evident in the range of relatively small loads that the experiment was conducted for; however, as bigger loads are exerted on the seat, this discrepancy is expected to decrease and the seat's effective spring constant is expected to converge to the stiffer pad's one. Therefore, a reasonable suggested estimate for the seat's (i.e. the 1 1/4" slab of the "EPC" foam topped with a 3/4" piece of the Polyester 4 lb density foam) overall effective spring constant in the human weight range is 75 lb/in.

3) for the Polyurethane foam pad

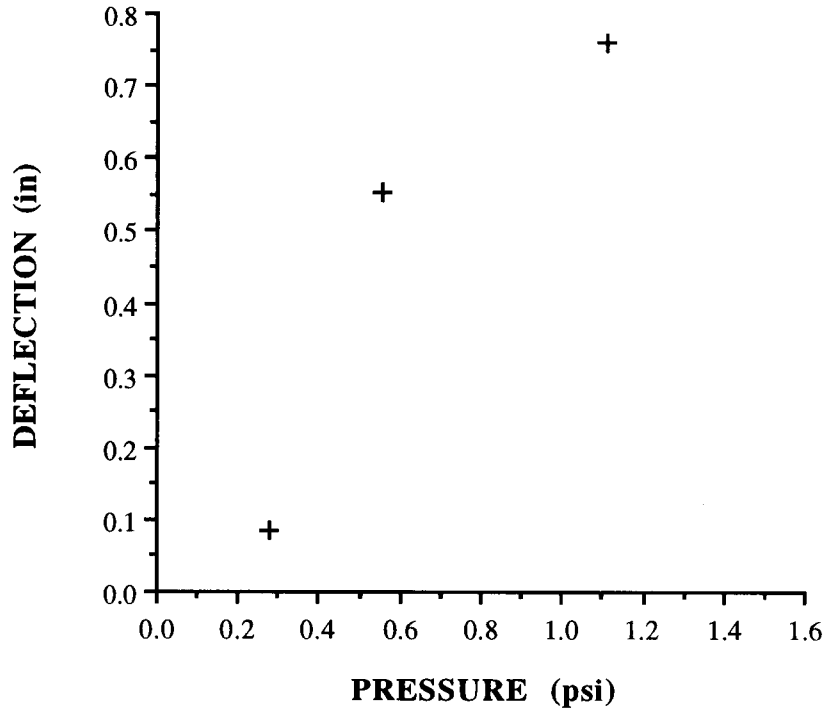

FIGURE 14 Polyurethane foam pad's deflection vs pressure.

Finally, as already mentioned, a new Polyurethane foam material suggested for BikeE's latest seat version was tested, revealing a spring constant of 21.6 lb/in before it gets squeezed flat with no major further deformation at a load of approximately 10 pounds. This result is also evident while riding the bicycle, as a poorer vibration isolation is experienced with the new suggested material. Given, however, the other advantages that the new foam pad has over the old one, a thicker layer of this material might provide a better combination of results and it would be interesting to be tested.

3.6 BIKEE's EXPERIMENTALLY RECORDED RESPONSE TO A 3/4" STEP BUMP

3.6.1 Introduction

The purpose of this experiment was to obtain the actual response of the bicycle as it drops down a 3/4" step bump in the form of its acceleration history. After the spring constants and damping coefficients of BikeE's different parts were determined experimentally, the acceleration history of its frame and passenger as it drops down a bump could help compare it with similar computer response simulations. Then, it would be possible to determine the suspension parameters that produce the best response possible by just changing these parameters on the computer and observing the resulting bicycle response. In other words, if the computer model seems to accurately represent the bicycle's actual response to bump excitation it could then be used to determine the spring constant and damping coefficient of a suspension system that would provide an "ideal" (or the closest to "ideal" possible) passenger response/ride.

3.6.2 Procedure

A PCB accelerometer kit was obtained and a 302A accelerometer (serial no. 11452) was used. The bicycle was driven up a 3/4" wooden plate, and a 100lb weight was placed and balanced on the bicycle's seat to simulate a riding passenger as shown in Figure 15. The accelerometer was then mounted on the bicycle's frame, directly above the rear wheel's center, and connected to a Tektronix 2211 digital storage oscilloscope. The

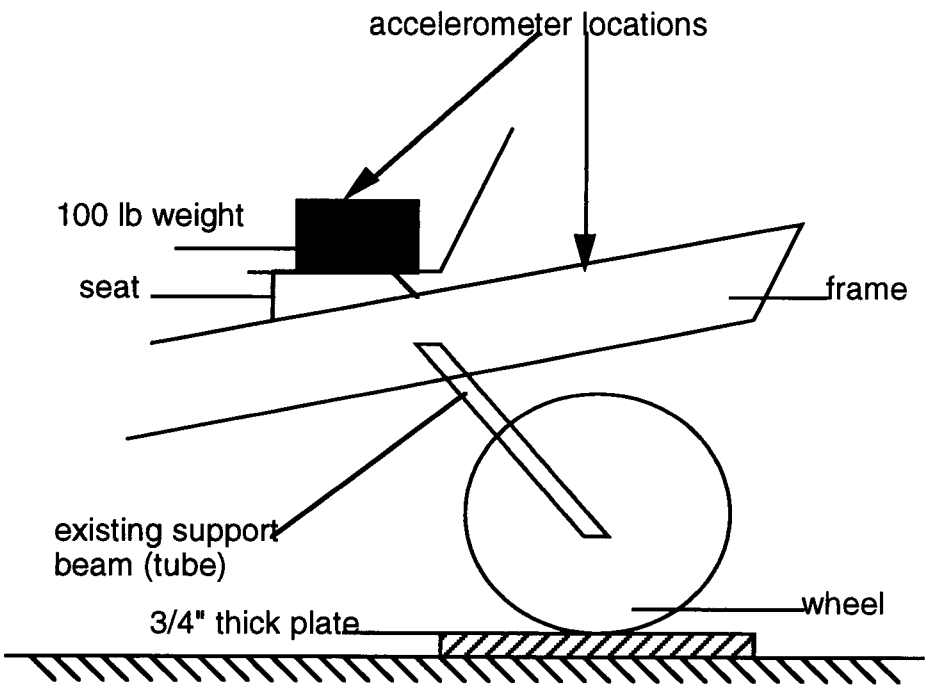

FIGURE 15 Figure of accelerometer placement and experimental apparatus.

oscilloscope was in turn set to an appropriate triggering level and connected to a Tektronix HC100 color plotter. As the bicycle was slowly driven down the 3/4" plate, its response (accelerometer signal) to the artificial bump was recorded on the oscilloscope. The experiment was run several times to establish data consistency, and a representative sample acceleration curve was printed. After the acceleration history of the bicycle's frame was obtained, the 302A accelerometer was mounted on the 100lb weight on the bicycle's seat, and an acceleration plot for the rider was similarly obtained.

3.6.3 Results

The acceleration history plots obtained are illustrated in Figures 16 and 17 that follow:

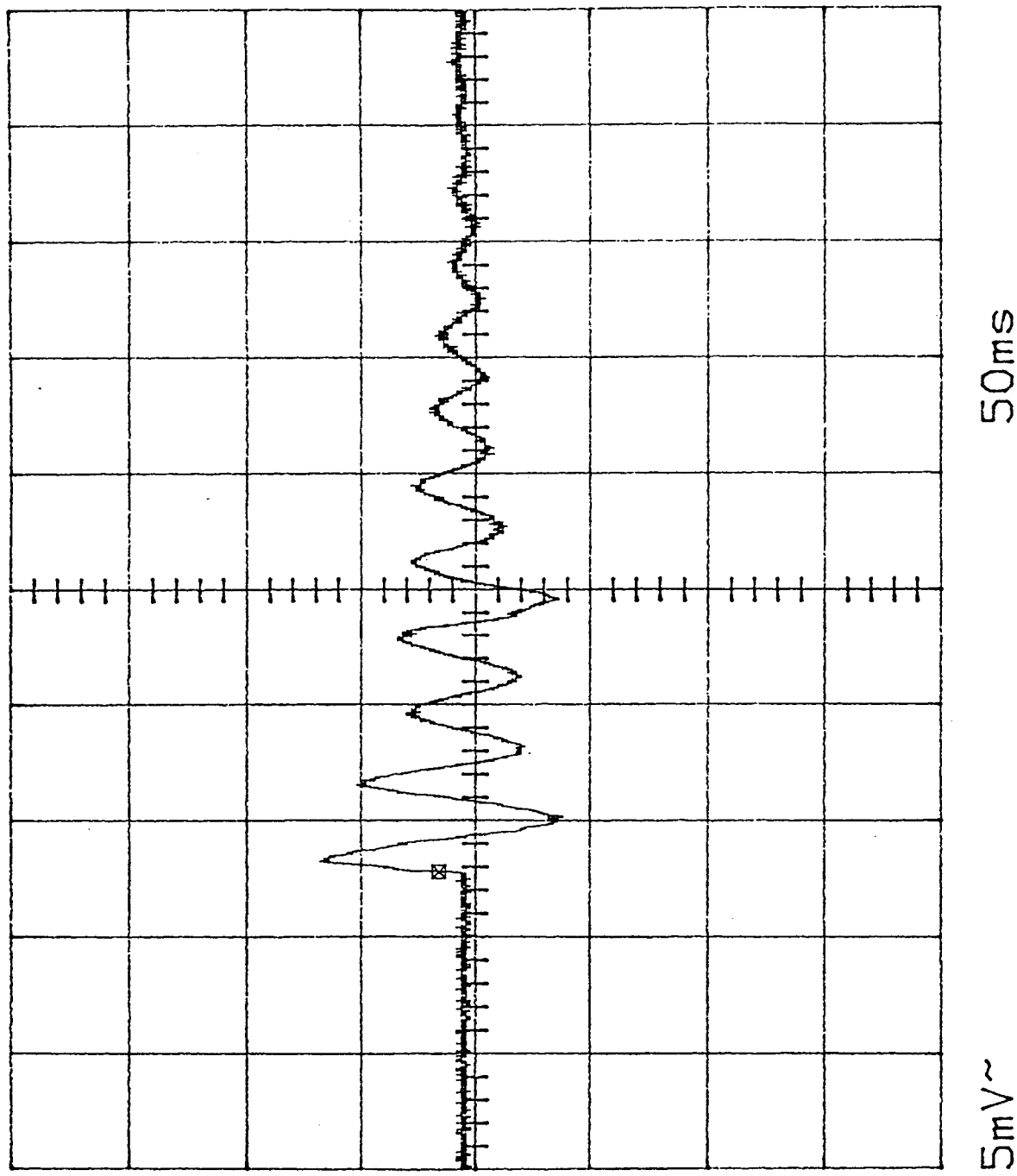

FIGURE 16 Frame response to a 3/4" step bump.

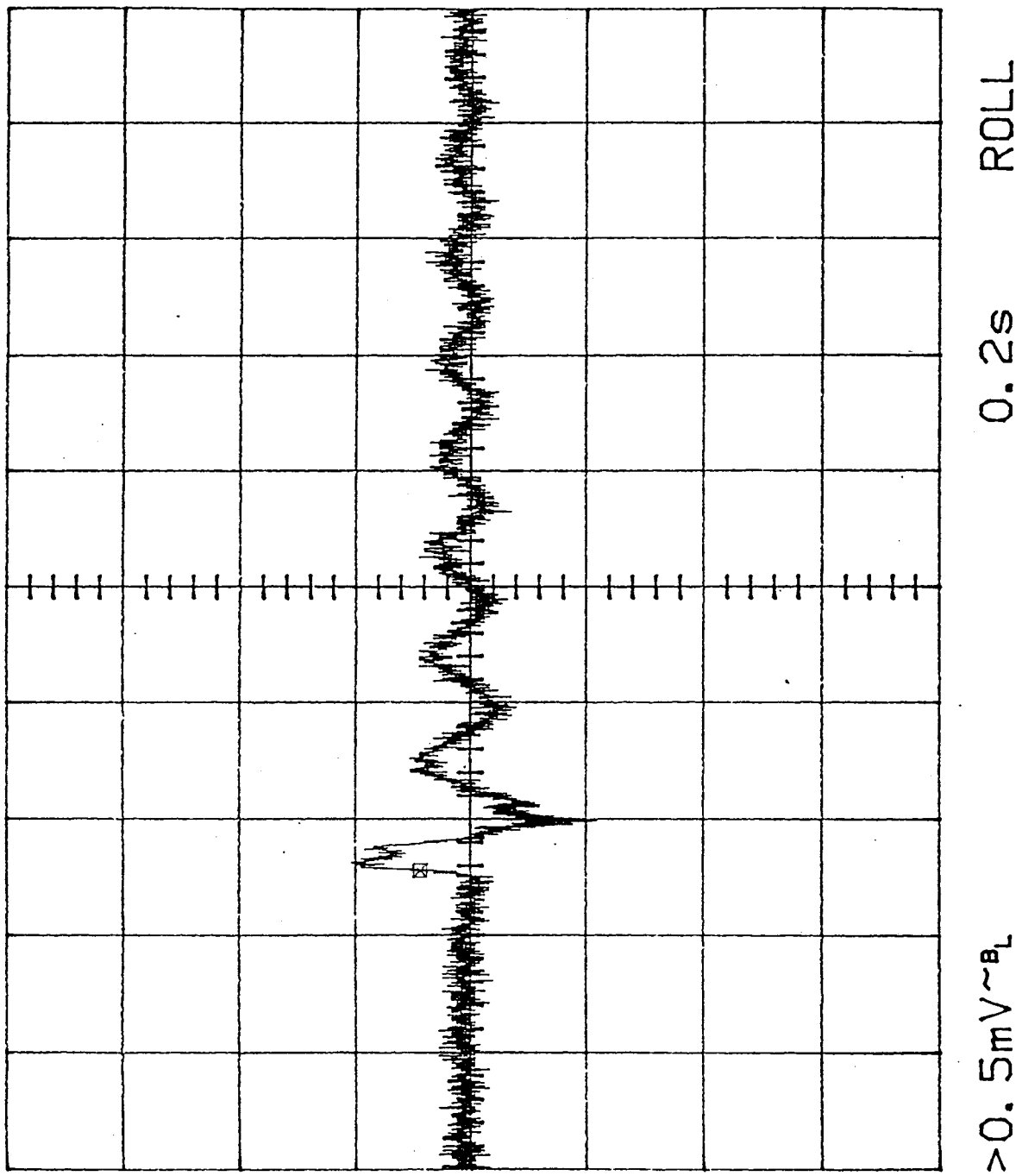

FIGURE 17 Seat/rider response to a 3/4" step bump.

3.6.4 Conclusions and Discussion of results

The 302A accelerometer's sensitivity is, as given by the manufacturer, approximately 10 mV/g. Hence, from the two acceleration history curves of section 3.6.3 (Figures 16 and 17) it can be calculated that the bicycle frame is experiencing a maximum vertical acceleration of 3g as it drops down a 3/4" bump, while the 100 lb rider is experiencing a maximum vertical acceleration of 0.25g for the same excitation drop.

Furthermore, the damping on the frame's response is, according to the corresponding acceleration curve (Figure 16,) 0.3 lb sec/in while the period of its response is approximately 1 second. This damping coefficient suggested for the bicycle's frame was calculated using the Logarithmic Decrement-Damping Ratio procedure explained in detail in section 3.4.4, and can be used for drawing some interesting conclusions about the rear wheel's damping properties. Since the damping capacity of the steel and aluminum parts of the bicycle's frame is relatively small (Whitt and Wilson, 1974), it is understood that the frame's damping of 0.3 lb sec/in is mainly in the rear wheel. In section 3.4.4 the rear wheel's damping coefficient was measured for different tire pressures (Table 9, Figure 10.) The bicycle's response to a 3/4" step drop experiment was conducted at a back tire pressure of approximately 35 psi, which corresponds to a rear wheel damping coefficient of 0.17 lb sec/in as the data of section 3.4.4 suggests. These two results, i.e. the value for the rear wheel's damping coefficient obtained in section 3.4.4, and the value suggested by the frame's acceleration history curve, are in good agreement with each other considering the additional damping (small, but still some) provided by the bicycle's frame and the spring-like 45^{o} angle rear stay.

On the other hand, the seat/rider acceleration history curve, illustrated in Figure 17, suggests that the corresponding damping coefficient of the whole bicycle is 0.6 lb sec/in while the period of its response is approximately 0.15 seconds. Again, the calculation of the damping coefficient of the whole bicycle assemly was based on the Logarithmic Decrement-Damping Ratio procedure presented in section 3.4.4, and can be used to draw some interesting conclusions about the damping properties of the seat's foam material. As the damping capacity of the seat's foam is clearly considerably higher than the ones of the other bicycle components, it is understood that most of the bicycle's 0.6 lb sec/in damping job is mainly performed by the seat's foam material. Hence, the seat foam's effective damping coefficient can be estimated to lie in the 0.5 to 0.6 lb sec/in range.

3.7 COMPUTER MODEL vs EXPERIMENTAL DATA

3.7.1 Introduction

After the experimental data on BikeE's response to a 3/4" step drop was obtained in section 3.6, a computer simulation for the same excitation drop of the bicycle was attempted in order to determine the extent of agreement between the laboratory and the computer generated results. A sufficient agreement would allow further experimentation on the computer on different suggested suspension system constants and locations in order to determine which combination would produce the best possible results, i.e. which combination would satisfy the customer requirements that were set for the suspension system in section 2.1 best.

3.7.2 Procedure

The computer program *Mathematica* was used to tackle the problem as it demonstrates a great flexibility in solving complex mathematical problems. More specifically, the NDSolve function/command that has the ability to solve a system of simultaneous ordinary differential equations and find its numerical solution was applied. The way NDSolve works is explained below:

NDSolve[{eqn_1, eqn_2, ...}, {y_1, y_2, ...}, {x, x_{min}, x_{max}}]

finds the numerical solutions for all the functions $y_i(x)$. This is done iteratively. NDSolve starts at a specific value of the independent variable x, and then takes a sequence of steps that eventually cover the whole range x_{min} to x_{max}. The solutions are, then, represented as "InterpolatingFunction" objects that provide approximations to the $y_i(x)$ functions over the range of x_{min} to x_{max}.

Next, the three equations of motion as well as the initial conditions that govern the wheel-frame-seat bicycle assembly, as a system of three spring-dampers one on top of the other, for a 3/4" step drop excitation were set up.

Equations Of Motion:

$$M_W x'' + (c_W + c_f)x' + (K_W + K_f)x - c_f y' - k_f y = (3/4)K_W \qquad (3.7.1)$$

$$M_f y'' + (c_f + c_s)y' + (K_f + K_s)y - c_s z' - K_s z - c_f x' - K_f x = 0 \qquad (3.7.2)$$

$$M_s z'' + c_s z' + K_s z - c_s y' - K_s y = 0 \qquad (3.7.3)$$

Initial Conditions:

$$x(0) = 0 \qquad (3.7.4)$$

$$x'(0) = 0 \qquad (3.7.5)$$

$$y(0) = 0 \qquad (3.7.6)$$

$$y'(0) = 0 \qquad (3.7.7)$$

where x(t), y(t) and z(t) represent the vertical displacements of BikeE's wheel, frame and seat with time, while

M_W is the mass of BikeE's rear wheel,
M_f is the mass of BikeE's frame,
M_S is the mass of the seat and the rider,
K_W is the rear wheel's spring constant,
K_f is the frame's spring constant,
K_S is the seat foam's spring constant,
c_W is the rear wheel's damping coefficient for a 35 psi tire pressure,
c_f is the frame's damping coefficient, and, finally,
c_S is the seat foam's damping coefficient.

The purpose of the computer simulation was, as mentioned above, to investigate the extent of the agreement between the computer generated results and the experimentally recorded ones in section 3.6 for the bicycle's response to a 3/4" step drop. Hence, before equations 3.7.1 to 3.7.7 were entered into the computer program, their characteristic constants were assigned values simulating the properties of BikeE's components and the laboratory conditions during its 3/4" step drop test described in section 3.6.

These values were, as expected, based on or calculated by the experimental results of all the tests conducted on BikeE's different parts earlier (sections 3.2 to 3.6), and taken to be:

W_W = the rear wheel's weight = 31.5 lb,
W_f = the frame's weight = 3.5 lb,
W_S = the seat/load's weight = 100 lb,
K_W = 500 lb/in, (from section 3.2.4)
K_f = 1500 lb/in, (from section 3.2.4)
K_S = 75 lb/in, (from section 3.5.4)
c_W = 0.17 lb sec/in, (from section 3.4.4)
c_f = 0.075 lb sec/in, and, finally, (from section 3.6.4)
c_S = 0.5 lb sec/in. (from section 3.6.4)

The program was then run, and the computer generated plots of the frame's and rider's acceleration history with time were obtained.

3.7.3 Results/Discussion of results

The acceleration history plots that were generated by the computer for both the bicycle's frame and the seat/rider system are shown respectively in Figure 18.

These plots were then compared to their corresponding, experimentally obtained ones that are illustrated in Figures 16 and 17 of section 3.6 respectively. It is evident that there is a very small, if any, agreement between the computer and experimental results in terms of the maximum amplitude, the damping, as well as the period of the respective

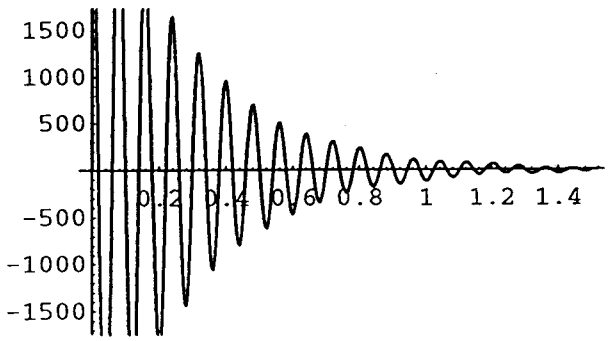

-Graphics-

a) Frame response.

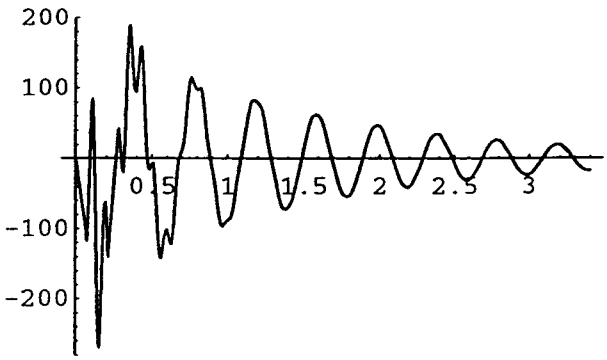

-Graphics-

b) Seat/rider response.

FIGURE 18 BikeE's frame and seat/rider computer generated response to a 3/4" bump.

responses. A possible reason for this discrepancy is the inadequacy of the 3 Degree of Freedom (DoF) linear model of three spring-dampers in series that was used to accurately describe the mechanics behind the bicycle's response to road surface excitation. Several different models of spring-damper combinations and configurations of variable complexity have occasionally been introduced to represent and approximate the shock absorption properties and behavior of materials and/or systems (Whitt and Wilson, 1974, and Wong, 1978.) The results of the computer simulation described in this section indicate that, although the 3 DoF model that was employed is sufficient for the analysis of the spring and damping properties of the bicycle's individual suspension components, it cannot adequately represent the way these components interact and respond to road bump excitation as a whole.

This unexpected discrepancy demonstrated the need for an even further, more detailed investigation of the road behavior properties of some of BikeE's suspension components. As a solution to this problem, the design of a testing apparatus that would allow the accurate determination of the more complex and/or hard to measure characteristic properties of the bicycle's rear wheel and seat, such as their spring constants and damping coefficients, was decided. The design and development of such a damping coefficient-spring constant test machine is presented in the next chapter.

4. DESIGN OF A DAMPING COEFFICIENT-SPRING CONSTANT TEST MACHINE

4.1 INTRODUCTION

The process of attempting to understand, and then successfully model, BikeE's road behavior by looking at its individual components and investigating their own function revealed the need for a dependable apparatus that could provide accurate information about the more complex and/or hard to measure characteristic properties (damping coefficient, spring constant) of some of these components. Furthermore, it also became evident that in designing such a device one of the most important goals was to try to achieve a relative "universality" of its experimental functions; in other words, a laboratory apparatus needed to be designed that would have the ability to measure the damping coefficients and spring constants of not only certain parts of the recumbent bicycle under investigation, but of a greater variety of materials and parts used (or to be used) in the bicycle industry. This way, such a testing device would be able to serve three purposes:

a) provide valuable information on specific projects related to the analysis and/or improvement of BikeE's performance,

b) test the performance of a wide range of competitive products in the market,

and finally,

c) assist in the investigation of the relative properties of various materials of interest before their industrial integration.

4.2 INITIAL STAGES OF THE DESIGN PROCESS

4.2.1 Determining the Customer Requirements/Design Criteria for the damping coefficient-spring constant test machine

The most important part of any design process is, as explicitly analyzed in section 2.1, the progressive, step-by-step development of a product from levels of high conceptual abstraction to better defined ones. This way the designer can achieve a better, gradual understanding of how the future product needs to function and interact with its surroundings. The exact steps that such a progressive product development should follow were defined and explained in length in section 2.1. There, they set the guidelines for the initial stages of the design of a suspension system for BikeE; here, they were used to assist in the design of a damping coefficient-spring constant test machine as described below.

Keeping in mind that the only customers of such a test machine are the machinist who is going to build it and the engineer who is going to operate it in the laboratory, the customer requirements for the test machine were defined in terms of its desired functions and properties. According to them, the test machine to be designed needs to:

1] Provide data that will allow the determination of the specimen's damping coefficient (range of interest: 0.05 to 0.8 lb sec/in)

2] Provide data that will allow the determination of the specimen's spring constant (range of major interest: 10 to 1000 lb/in)

3] Be able to be used for testing both different seat materials and bicycle wheels

4] Be able to provide data for different impact loads

5] Be as accurate and precise as possible

6] Operate affected by frictional energy losses as little as possible

7] Be affected by environmental and other external factors as little as possible

8] Be easy to manufacture

9] Be easy to assemble

10] Be easy to transport

11] Be easy to understand and operate

12] Be safe to operate and transport

13] Have a long life span

14] Be environmentally friendly

15] Provide a flexibility for a greater variety of specimen testing

All the customer requirements listed above also served, just like the ones in the suspension system case in section 2.1, as the design criteria for the evaluation of the different design concepts to evolve in later design stages. Hence, after a weighting factor (again, in a scale from 1 to 10) was assigned to each one of them according to their relative importance, they were organized in the form of a decision matrix. The decision matrix for the test machine is shown on the next page (Figure 19.)

4.2.2 Literature review

After the damping coefficient-spring constant test machine's desired properties and functions were defined in the form of its customer requirements (section 4.2.1,) an extended literature search/review was conducted in order to investigate a) the existence of similar machines, and b) the corresponding practices followed for similar problems at both

	DAMPING COEFF.-SPRING CONSTANT TEST SYSTEM DECISION MATRIX	WEIGHT (scale 1-10)	CONCEPTS TO BE COMPARED						
			I	II	III	IV	V	VI	VII
CUSTOMER REQUIREMENTS / CRITERIA	Provide data that will allow the determination of the specimen's damping coefficient	10							
	Provide data that will allow the determination of the specimen's spring constant	10							
	Be able to be used for testing both different seat materials and bicycle wheels	8							
	Be able to provide data for different impact loads	8							
	Be as accurate and precise as possible	8							
	Operate affected by frictional energy losses as little as possible	7							
	Be affected by environmental and other external factors as little as possible	7							
	Easy to manufacture	7							
	Easy to assemble	6							
	Easy to transport	6							
	Easy to understand and operate	6							
	Safe to operate and transport	8							
	Long life span	6							
	Environmentally friendly	5							
	Flexible for a greater variety of specimens testing	6							
EVALUATION	OVERALL SCORE	TOTAL +							
		TOTAL -							
		NET TOTAL							
	WEIGHTED SCORE	TOTAL +							
		TOTAL -							
		NET TOTAL							

FIGURE 19 Decision Matrix for the damping coefficient-spring constant test machine.

experimental and industrial levels.

First, as far as damping coefficient measurements are concerned, there are basically two types of methods used for both laboratory and industrial purposes:

- The static testing ones, and
- The dynamic testing ones (Nashif, Jones, and Henderson, 1985.)

The static testing methods seem to be more widely used due to their relative simplicity with respect to the dynamic ones. There are three types of static tests that are commonly performed:

The cyclic load-deflection test

In this type of test, the specimen is loaded and unloaded through a complete cycle of tension and compression that consists of three steps: initial loading to some load +/- P_d, unloading to the opposite load -/+ P_d, and then reloading to the initial load (Harris and Crede, 1961.) The applied loads and their corresponding deflections are recorded, and then graphed. The resulting curve is the specimen's hysteresis loop, from which the damping coefficient can be calculated since the damping energy dissipated during one load-deflection cycle (between load limits +/- P_d or deflection limits +/- δ_d) is proportional to the area within the loop (ASA, 1976.)

The drop test

In this test, a load (usually a metal sphere) is dropped onto the specimen from a specific initial height, and its rebound height is measured. The damping ratio of the drop is then determined, which, in turn, allows the calculation of the specimen's damping coefficient. The drop test is the most widely used one for the measurement of the damping coefficients of

foams (The International Plastics Selector, 1978.)

The pendulum test

The pendulum test is by far the most commonly used one, especially in the automotive industry. It is, in principal, very similar to the drop test. In this case, a pendulum with a flat dropping head is let bounce off the specimen from a specific height-angle. The rebound angle of the pendulum is, then, measured, the damping ratio determined, and the specimen's damping coefficient is calculated exactly as in the drop test (The International Plastics Selector, 1978.)

On the other hand, the dynamic testing methods are more sophisticated both in terms of equipment, experimental set-up, and result analysis (ASTM, 1993.) In most of the cases that they are used, they function more as a way to cross-check and reconfirm results obtained from static tests (Korenev and Reznikov, 1993). Although different variations can be encountered, the basic principal behind dynamic testing methods is the periodic mechanical excitation of the specimen, and recording of its response by means of, usually, an accelerometer (Courtney, Charlton, and Seel, 1993.)

In the cases, now, where both damping coefficient and spring constant measurements are desired, the cyclic load-deflection test described earlier is used. The generation of the specimen's hysteresis loop does not only allow the calculation of its damping coefficient from the loop's area, but also provides sufficient information (namely the slope of the curve produced by the initial load-deformation results obtained during the test's first step) for the calculation of the specimen's spring constant. However, the cyclic load-deflection test requires the use of more sophisticated,

accurate, and expensive equipment than the other two static tests, and, for this reason, is usually used by large scale industrial manufacturers. It is the goal of the design endeavor described in this chapter to lead to the development of a simple to manufacture and operate, inexpensive test machine that can provide both damping coefficient and spring constant data for use at smaller scale laboratory and manufacturing levels.

4.2.3 First round of Decision Matrix Concept Evaluation

After the available literature on the subject was adequately explored, the actual design phase started. In light of the testing methods described in section 4.2.2, several test machine concepts were generated reflecting some design ideas still at a very abstract level. Some of them were based on the testing methods of the previous section, while the rest applied some more ambitious ideas like heat dissipation measurements and ultrasonics. The advantages and disadvantages of all these design concepts with respect to the design criteria established earlier were, then, evaluated by means of the decision matrix for the test machine (Figure 19) that was developed in section 4.2.1. When the first round of the decision matrix concept evaluation was completed, the idea that emerged as the one presenting the highest potential for a successful product design and development was the one closely resembling the Pendulum Test of section 4.2.2.

4.3 FINALIZING THE PRODUCT DESIGN

With the "pendulum" concept clearly being the favorite after the first decision matrix round, the next step was to try to develop new ideas

around it, progressively moving to less abstract stages of the design process (Conklin and Yakemovic, 1991.)

The most critical parts/features of a pendulum-like apparatus, designed to function as a damping coefficient-spring constant test machine are:

a) the orientation (horizontal or vertical) of the pendulum's impact position

b) the pendulum's support (i.e. what is the pendulum attached to and how)

c) the pendulum's pivot point location with respect to its support

d) the shape and size of the pendulum's dropping head, and

e) the specimen mounting device

So, a variety of pendulum-based design concepts were developed, each one mainly focusing on a different idea around the features addressed above, and, again, weighted against each other in a second round of decision matrix evaluation. The concept that appeared to satisfy the already set customer requirements/design criteria best was, then, selected to serve as the basis for the test machine's final design. After a careful last touch of refinement and improvement, the ultimate stage of the test machine's design process was concluded and its final product was put in the form of the two AutoCAD drawings illustrated in Figures 20 and 21.

The structure of the proposed damping coefficient-spring constant Pendulum test machine, as well as the idea behind it, is relatively simple. It basically consists of two major parts: the pendulum itself (Figure 20,) and its base of operation (Figure 21.) Each of these two parts is made up of its own individual elements. All the parts of the Pendulum test machine are described below:

The pendulum, first, consists of the following six components:

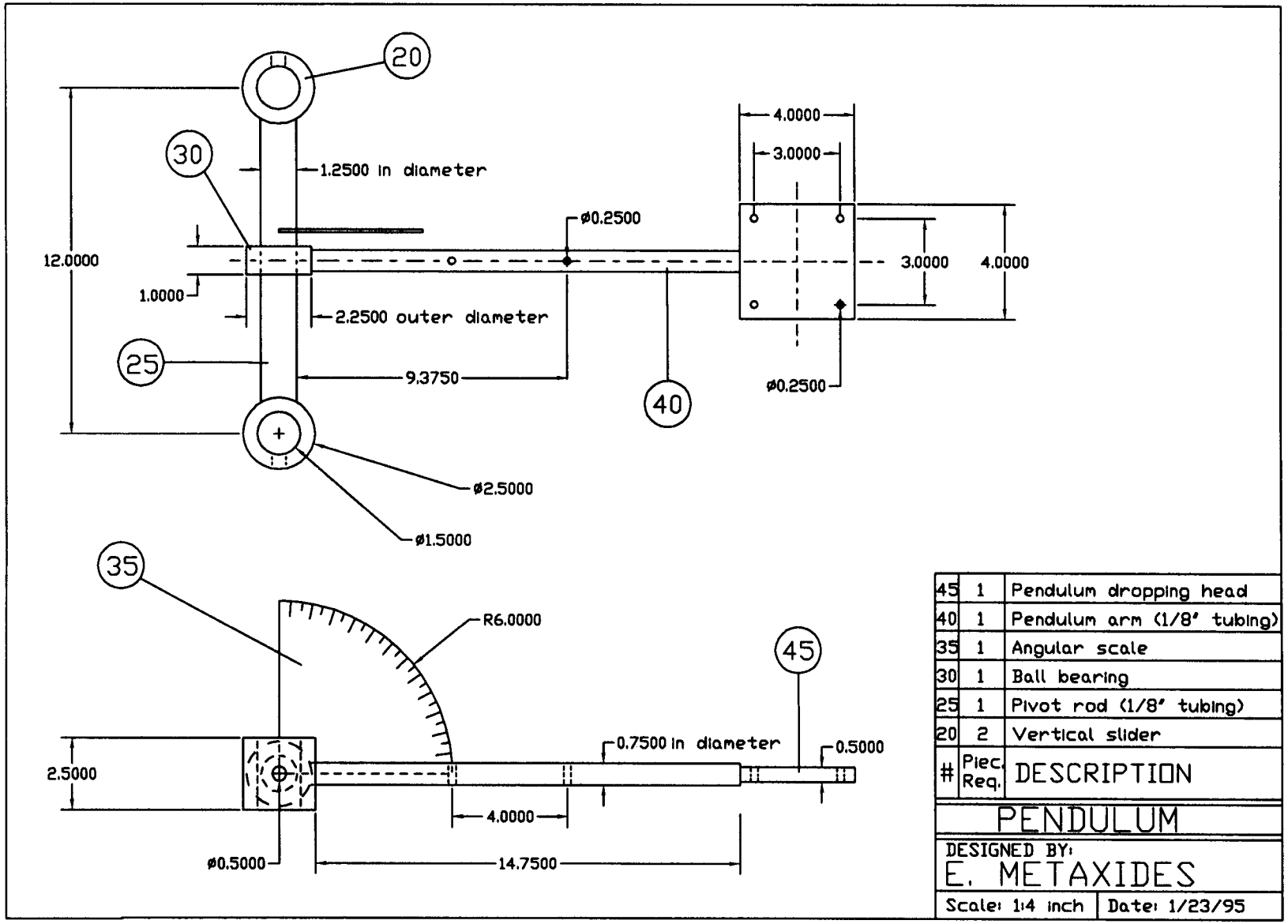

FIGURE 20 The Pendulum.

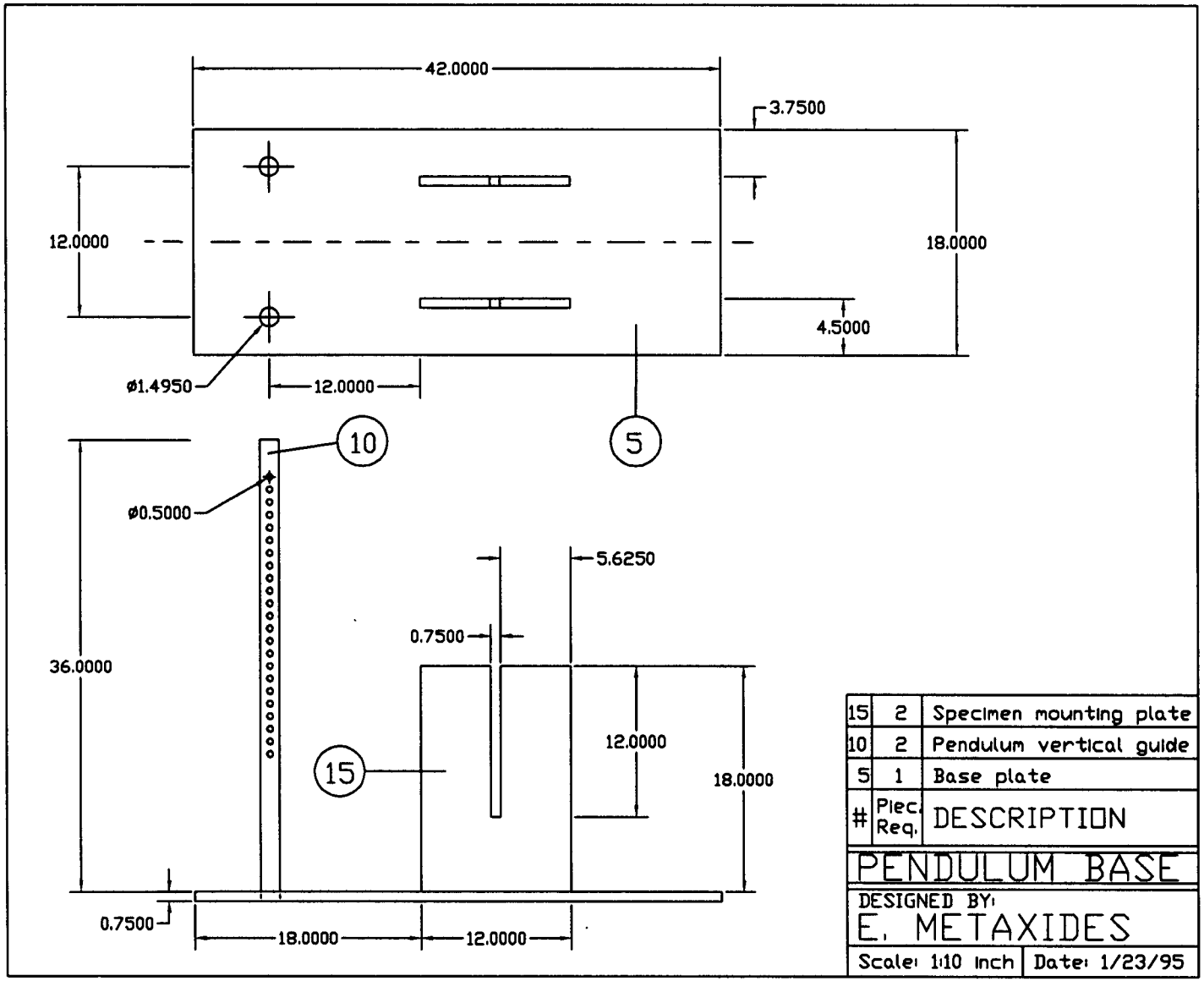

FIGURE 21 The Pendulum's base.

1] **The dropping head**, a 4"x4" aluminum plate with a thickness of 1/2". It carries four 1/4" diameter holes located at the four corners, 1/2" from each side of the plate. These holes serve as means of additional weight attachment onto the dropping head when a greater impact load is desired, or when the machine is used for load-deflection measurements.

2] **The pendulum arm**, a $14\frac{7}{8}$" long aluminum rod directly attached to the pendulum's dropping head. It has a 3/4" diameter and an 1/8" tubing. Two 1/4" diameter holes are drilled symmetrically about the rod's middle point, 4" apart, for the mounting of a bench level along the arm's axis.

3] A **ball bearing** with an $1\frac{1}{4}$" inner diameter and 1" axial length. The ball bearing is very tightly surrounded by an aluminum cylindrical cover shell where the also aluminum pendulum arm is welded on. This way the pendulum arm can freely spin around the ball bearing's axis. The combined outer diameter of the fixed ball bearing-cylindrical cover assembly is $2\frac{1}{4}$".

4] **The pendulum's pivot rod**, a $9\frac{1}{2}$" long aluminum tube around the middle of which the ball bearing's inner ring surface is fixed. It is $1\frac{1}{4}$" in diameter with an 1/8" tubing.

5] An **angular scale**, attached to the pivot rod, for the measurement of the pendulum's rebound angle with respect to the initial drop angle, and finally,

6] Two **cylindrical sliders**, connected to each other by the pendulum's pivot rod. They are made of aluminum also, and can slide simultaneously along two vertical shafts. Hence, besides establishing a greater vertical operational range for the pendulum assembly, these two sliders provide the apparatus with the essential vertical deflection flexibility when load-deflection measurements are conducted. They both have an outer diameter of $2\frac{1}{2}$" and an inner diameter of $1\frac{1}{2}$". Their axial length is $2\frac{1}{2}$", and they both carry a 1/2" diameter hole which is coaxial with the pendulum's pivot rod.

On the other hand, the pendulum's base consists of three parts:

1] **The base plate**, a 18"x42" cast iron plate with a uniform thickness of 3/4". It carries two 1.495" diameter holes that are both drilled at 6" from one of the plate's shorter sides, 12" apart.

2] **The vertical guides**, two $36\frac{3}{4}$" long solid rods along which the

pendulum's cylindrical sliders can move freely. They are made of steel and are press-fit into the base plate's 1.495" diameter holes. Several pairs of coaxial 1/2" diameter holes are drilled symmetrically through the respective rods facing each other. The distance between adjacent holes on each rod is 1 inch. These holes function as the cylindrical sliders' locking device onto the vertical guides. This is accomplished by means of two metal pins that can be inserted through the sliders' 1/2" diameter holes into the corresponding ones on the vertical guides when the pendulum's desired height is determined.

3] Finally, **the mounting plates**, two 12"x18" cast iron plates that are welded 9" apart on the test machine's base plate. They are both 3/4" thick, and are positioned symmetrically with respect to the pendulum base's axis of symmetry. They both carry a vertical 3/4" wide slip that runs 12" down the middle of their top surface, where the specimen to be tested (or its support) is inserted, positioned at the desired height, and secured. The mounting plates also ensure that, before testing, the specimen's center is directly below the dropping head's center when the pendulum arm is at a horizontal position.

As mentioned earlier, the concepts behind the Pendulum test machine's design and way of operation are fairly simple. First, its function as a damping coefficient test machine is based on the measurement of the pendulum arm-dropping head system's rebound angle with respect to the initial drop angle, after it bounces off the specimen under testing. With the pendulum's rebound and initial drop angle both at hand, the specimen's damping coefficient can then be computed by following the Logarithmic Decrement-Damping Ratio procedure presented in section 3.4. However, before a pendulum drop test is ready to be conducted, a series of several preparatory steps needs to be followed. Initially, the specimen to be tested (a foam material suggested for use in a bicycle seat, a bicycle wheel, ETC.) is properly positioned and secured onto the specimen mounting plates. Then, the pendulum arm is brought to rest on the specimen at a horizontal position with respect to the specimen's top surface. This is achieved by

moving the cylindrical sliders vertically along their guides and/or adjusting the height of the specimen's position on the mounting plates. The pendulum's horizontality is established by means of a bench level attached along the pendulum arm. The two cylindrical sliders are then locked onto their respective vertical guides, and the pendulum head is released to drop freely onto the specimen from a pre-determined[1] angle/height. Its rebound angle is measured by means of an angular scale attached to the pendulum's pivot rod.

On the other hand, the test machine's function as a spring constant measuring device is based on obtaining a sufficient set of load-deflection data about the specimen whose elastic properties are under investigation. After an adequate set of load-deflection data is obtained, the specimen's spring constant can be determined by plotting the recorded load-deflection measurements and calculating the slope of the resulting curve. Again, before performing a spring constant measurement test, the specimen needs to be properly placed and secured on the mounting plates, and the pendulum arm needs to be positioned on the specimen at a horizontal position with respect to the specimen's top surface. The two cylindrical sliders are then locked onto their respective vertical guides, and different weights can be gradually attached to the pendulum's dropping head for measuring the specimen's corresponding vertical deflection. The specimen's vertical deflection under load is measured by slowly lowering the pendulum arm (by means of the vertical sliders) until it reaches a horizontal position, and/or adjusting the height of the specimen's position

---

[1] For similar tests at the industrial level, R & D groups have developed different specimen type/thickness versus recommended drop height reference tables according to their individual needs and specimen type.

on the mounting plates. The pendulum's horizontality is always established using the bench level on the pendulum arm. Vertical deflection versus load data can also be obtained for equal deflection steps by gradually (one notch at a time) lowering the pendulum along the vertical guides, and attaching additional weights onto the dropping head until the bench level indicates that a horizontal position has been reached each time.

5. CONCLUSIONS AND RECOMMENDATIONS

5.1 CONCLUSIONS

Due to the dual nature of this study (i.e. the design of a damping coefficient-spring constant test machine, in association with the static and dynamic testing of BikeE's suspension components as part of a suspension system design process), the conclusions that can be drawn from all the presented results are of two different kinds themselves. The first kind is related to the purely experimental results obtained in Chapter 3 as products of BikeE's testing. The other kind, more abstract in nature, is associated with the results acquired and the experiences gained from both design issues involved in this study.

The conclusions that can be derived from the experimental results of all the static and dynamic tests performed on BikeE are really relevant to the properties of BikeE's suspension components only. However, useful inferences can be drawn from them about the response to road surface excitation exhibited by similar suspension parts used not only for BikeE's latest models, but other types of bicycles as well. These conclusions, individually discussed in detail at the end of sections 3.2 through 3.6, are summarized below in the order they were presented in Chapter 3:

1] The spring constant of BikeE's rear wheel is 458.2 +/- 16.7 lb/in, while the spring constant of its frame is 1519.7 +/- 15% lb/in.

2] The maximum strains that develop under load on BikeE's rear stay increase linearly with load, following - on the average - the

relationship:

$$|Strain_{max}| \text{ (in microstrains)} = 15.0 \times Load_{applied} \text{ (in pounds)}$$

as the slopes of the strain-load curves indicate.

3] The damping coefficient of BikeE's rear wheel is 0.18 lb sec/in at a tire pressure of 30 psi and 0.10 lb sec/in at a tire pressure of 65 psi, exhibiting a linear behavior within this tire pressure range.

4] The overall effective spring constant of BikeE's two foam layer seat in the human weight range is 75 lb/in.

5] The maximum vertical acceleration experienced by BikeE's frame while it drops down a 3/4" step bump is 3g, while a 100 lb rider on it experiences a maximum vertical acceleration of 0.25g for the same excitation drop.

6] The damping on the bicycle frame's response to a 3/4" step drop is 0.3 lb sec/in with a response period of 1 second, while the damping coefficient of the whole bicycle is 0.6 lb sec/in and its response period 0.15 seconds for the same excitation drop.

7] The effective damping coefficient of BikeE's two foam layer seat lies in the 0.5 to 0.6 lb sec/in range.

On the other hand, the "creative" aspect of this study led to the design of a testing device that can be used for damping coefficient and spring constant measurements; a testing device that is simple to manufacture, operate, and employ for data acquisition purposes at all research levels. In addition, the exposure to the design demands and experiences associated with this project led also to very useful conclusions regarding the nature of Design itself. Nothing could describe these conclusions more accurately than the following statement by Professor David G. Ullman of Oregon State University as it appears in his book "The Mechanical Design Process."

"Creativity takes hard work and can be aided by good design procedures."

Good design procedures (like the ones described in sections 2.1 and 2.2) allow the designer to achieve a complete, well-rounded understanding of the most fundamental objective during the initial design stages, which is to know what exactly needs to be developed; hard work ultimately provides him/her with valuable knowledge and experience to accompany his/her creative talents and help refine them.

5.2 RECOMMENDATIONS/SUGGESTIONS FOR FURTHER FUTURE RESEARCH AND USE OF THE PRESENTED RESULTS

With the design of the damping coefficient-spring constant Pendulum test machine completed (Chapter 4,) the next research priority is the implementation of these design results to fulfill the needs that led to their creation, i.e.

- the use of the Pendulum test machine to confirm the experimentally obtained results on the suspension properties of BikeE's components, and provide similar data for the parts that were not extensively tested.

During the course of this study, in addition to the research objectives already discussed, several other issues emerged either as sources of potential problems or merely as subjects of scientific interest. These issues, associated with either the damping and elastic properties of BikeE's individual suspension components or the bicycle's overall response to surface road excitation, give rise to some interesting questions worth of further investigation in the future. The study and analysis of these questions becomes even more intriguing in light of the development of the damping coefficient-spring constant Pendulum test machine which can

provide very useful information around them. A concise list of the potential future research subjects related to this study is given below:

- A detailed investigation of the way the damping coefficient of BikeE's rear wheel varies with tire pressure, performed for a greater range and sample number of tire pressures than the experiment presented in section 3.4.
- A thorough investigation of the damping coefficients and spring constants of a wide variety of types and sizes of foam materials for BikeE's seat, as means of determining the combination with the best response to road bump excitation.
- Testing, in terms of their suspension characteristics and shock absorption performance, and relative evaluation of BikeE's benchmarks and market competition.
- Finally, development of a spring-damper model and a corresponding computer simulation that can accurately represent BikeE's response to road surface excitation, and could be used for further analysis and improvement of the bicycle's road performance.

BIBLIOGRAPHY

ASA, STD 6-1976. 1976. *Nomenclature for Specifying Damping Properties of Materials.* ASA.

ASTM, Designation: E 756-93. 1993. *Standard Test Method for Measuring Vibration-Damping Properties of Materials.* ASTM.

Conklin, J., and Burgess Yakemovic. 1991. *A Process-oriented Approach to Design Rationale.* Human-Computer Interaction, Fall 1991.

Courtney, M. H., L. J. Charlton, and K. Seel. 1993. *Influence of Foam Density on Automobile Seat Performance.* SAE.

Harris, Cyril M., and Charles E. Crede. 1961. *SHOCK and VIBRATION HANDBOOK.* McGraw-Hill Book Company, Inc.

Housner, George W., and Donald E. Hudson. 1980. *Applied Mechanics and Dynamics*, 2nd edition. California Institute of Technology Press.

Housner, George W., and Thad Vreeland Jr. 1983. *The analysis of stress and deformation*, 5th reprint. California Institute of Technology Press.

The International Plastics Selector, Inc. 1978. *FOAMS*, desk-top data bank. Cordura Publications, Inc.

Korenev, Boris G., and Leonid M. Reznikov. 1993. *Dynamic Vibration Absorbers.* John Wiley & Sons Ltd.

Measurements Group, Inc. 1983. *Student Manual for Strain Gage Technology*, Bulletin 309A. Education Division: Measurements Group, Inc.

Nashif, Ahid D., David I. G. Jones, and John P. Henderson. 1985. *Vibration Damping.* A Wiley-Interscience Publication: John Wiley & Sons, Inc.

Ullman, David G. 1992. *The Mechanical Design Process.* McGraw-Hill, Inc.

Whitt, Frank R., and David G. Wilson. 1974. *Bicycling Science: Ergonomics and Mechanics.* The MIT Press.

BIBLIOGRAPHY (CONTINUED)

Wong, J. Y. 1978. *Theory of Ground Vehicles.*
A Wiley-Interscience Publication: John Wiley & Sons, Inc.